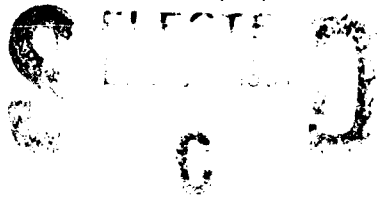

AFIT/GEO/ENG/91D-01

REAL IMAGERY AS A THREE DIMENSIONAL DISPLAY

THESIS

Juan C. Echeverry, Captain, USAF

AFIT/GEO/ENG/91D-01

DISCLAIMER NOTICE

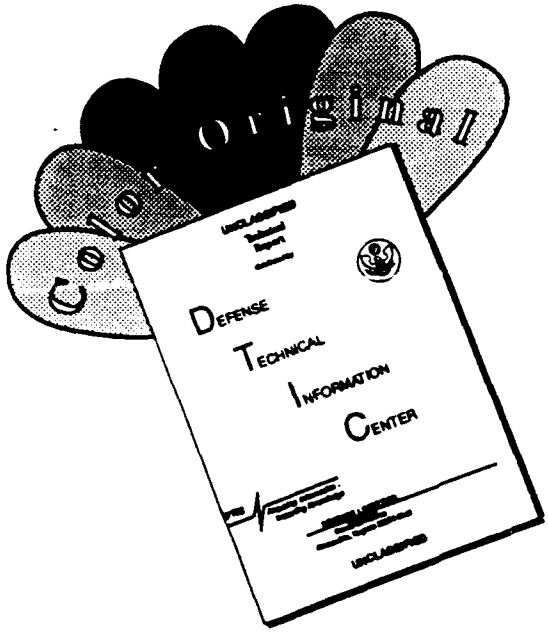

THIS DOCUMENT IS BEST QUALITY AVAILABLE. THE COPY FURNISHED TO DTIC CONTAINED A SIGNIFICANT NUMBER OF COLOR PAGES WHICH DO NOT REPRODUCE LEGIBLY ON BLACK AND WHITE MICROFICHE.

December 1991 *Master's Thesis*

Real Imagery as a Three Dimensional Display

Juan Carlos Echeverry, Capt, USAF

Air Force Institute of Technology, WPAFB OH 45433-6583 AFIT/GEO/ENG/91D-01

Approved for Public Release; Distribution Unlimited

This research effort implemented two 3-D display designs to assess their performance and effect on an observer's depth perception. Both 3-D displays produced real images for the observer to view. The first display setup combined a lens relay with a two concave mirror projector. The second display setup combined the two concave mirror projector with a diffuser. The lens relay/two concave mirror projector combination was successful in imaging a source from the CRT to a point in space above the two mirror system. The problem was that the observer could not assess the image location by just looking at it because it lacked concrete horizontal and vertical references for the observer to assess along with the image. The three-dimensional effect produced by the image could not be assessed easily because of the limited size of the image. The diffuser/two concave mirror combination was more successful as a display because it was comfortable to view. The design took advantage of the three-dimensional imaging that the two mirror system was already capable of generating. This design produced an image that the observer easily perceived as floating above the two mirror system. In essence, the image of the diffuser appearing at the top of the two mirror system acted as the horizontal and vertical reference that was lacking in the previous experiment. The use of depth cues in the image gave the observer the ability to interpret depth.

118

Three Dimensional Display; Real Imagery; Holographic Optical Element

UNCLASSIFIED UNCLASSIFIED UNCLASSIFIED UL

GENERAL INSTRUCTIONS FOR COMPLETING SF 298

The Report Documentation Page (RDP) is used in announcing and cataloging reports. It is important that this information be consistent with the rest of the report, particularly the cover and title page. Instructions for filling in each block of the form follow. It is important to **stay within the lines to meet optical scanning requirements.**

Block 1. Agency Use Only (Leave Blank)

Block 2. Report Date. Full publication date including day, month, and year, if available (e.g. 1 Jan 88). Must cite at least the year.

Block 3. Type of Report and Dates Covered. State whether report is interim, final, etc. If applicable, enter inclusive report dates (e.g. 10 Jun 87 - 30 Jun 88).

Block 4. Title and Subtitle. A title is taken from the part of the report that provides the most meaningful and complete information. When a report is prepared in more than one volume, repeat the primary title, add volume number, and include subtitle for the specific volume. On classified documents enter the title classification in parentheses.

Block 5. Funding Numbers. To include contract and grant numbers; may include program element number(s), project number(s), task number(s), and work unit number(s). Use the following labels:

C	- Contract	**PR**	- Project
G	- Grant	**TA**	- Task
PE	- Program Element	**WU**	- Work Unit Accession No.

Block 6. Author(s). Name(s) of person(s) responsible for writing the report, performing the research, or credited with the content of the report. If editor or compiler, this should follow the name(s).

Block 7. Performing Organization Name(s) and Address(es). Self-explanatory.

Block 8. Performing Organization Report Number. Enter the unique alphanumeric report number(s) assigned by the organization performing the report.

Block 9. Sponsoring/Monitoring Agency Names(s) and Address(es). Self-explanatory.

Block 10. Sponsoring/Monitoring Agency. Report Number. (If known)

Block 11. Supplementary Notes. Enter information not included elsewhere such as: Prepared in cooperation with...; Trans. of ..., To be published in .... When a report is revised, include a statement whether the new report supersedes or supplements the older report.

Block 12a. Distribution/Availablity Statement. Denote public availability or limitation. Cite any availability to the public. Enter additional limitations or special markings in all capitals (e.g. NOFORN, REL, ITAR)

DOD - See DoDD 5230.24, "Distribution Statements on Technical Documents."
DOE - See authorities
NASA - See Handbook NHB 2200.2.
NTIS - Leave blank.

Block 12b. Distribution Code.

DOD - DOD - Leave blank
DOE - DOE - Enter DOE distribution categories from the Standard Distribution for Unclassified Scientific and Technical Reports
NASA - NASA - Leave blank
NTIS - NTIS - Leave blank.

Block 13. Abstract. Include a brief (Maximum 200 words) factual summary of the most significant information contained in the report.

Block 14. Subject Terms. Keywords or phrases identifying major subjects in the report.

Block 15. Number of Pages. Enter the total number of pages.

Block 16. Price Code. Enter appropriate price code (NTIS only).

Blocks 17. - 19. Security Classifications. Self-explanatory. Enter U.S. Security Classification in accordance with U.S. Security Regulations (i.e., UNCLASSIFIED). If form contains classified information, stamp classification on the top and bottom of the page.

Block 20. Limitation of Abstract. This block must be completed to assign a limitation to the abstract. Enter either UL (unlimited) or SAR (same as report). An entry in this block is necessary if the abstract is to be limited. If blank, the abstract is assumed to be unlimited.

AFIT/GEO/ENG/91D-01

REAL IMAGERY AS A THREE DIMENSIONAL DISPLAY

THESIS

Presented to the Faculty of the School of Engineering

of the Air Force Institute of Technology

Air University

In Partial Fulfillment of the

Requirements for the Degree of

Master of Science in Electrical Engineering

Juan C. Echeverry, B.S.E.E

Captain, USAF

December, 1991

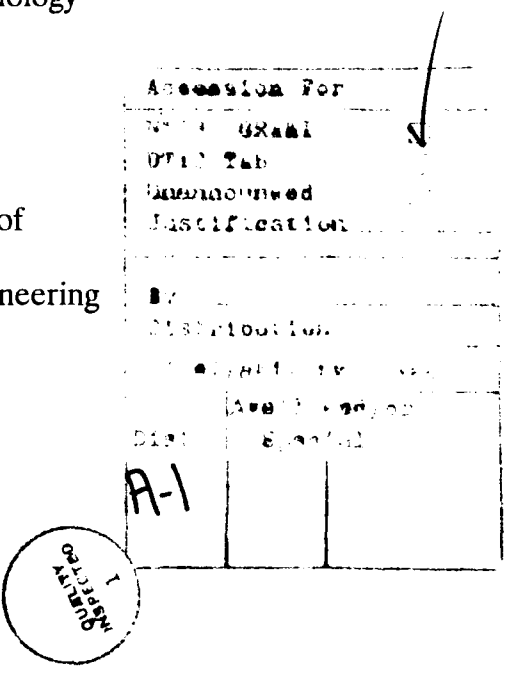

Preface

I would like to thank the many individuals that gave me the inspiration to persevere during this project.

My thesis advisor, Major Steve Rogers, gave me the determination to continue even at the height of confusion. He helped nurture the idea for this three dimensional display, and kept me from running rampant with complicated solutions. His imagination and inspiration made this research effort a rewarding one.

My thesis committee, Dr Matt Kabrisky and Lt Col Phil Amburn, both gave me the reinforcement I needed to believe that I was capable of producing successful results. I am grateful to Dr Kabrisky for exposing me to the wealth of his knowledge. It made this learning experience fun. I am also grateful to Lt Col Amburn for his help on the Silicon Graphics workstations, and most of all for his perpetual confidence that this project was not impossible.

I would like to thank all my fellow GEOs for helping me keep my perspective these past 18 months.

Most of all, I would like to thank my wife, Nadine, for giving so much of herself during this AFIT experience. Her love and support gave me the will to see this program to its end. And finally, Anthony, my son, thanks for giving me that special smile everytime I got away from my desk.

Juan C. Echeverry

Table of Contents

Page

List of Figures

List of Tables

Abstract

This research effort implemented two 3-D display designs to assess their performance and effect on an observer's depth perception. Both 3-D displays produced real images for the observer to view. The first display setup combined a lens relay with a two concave mirror projector. The second display setup combined the two concave mirror projector with a diffuser.

The lens relay/two concave mirror projector combination was successful in imaging a source from the CRT to a point in space above the two mirror system. The problem was that the observer could not assess the image location by just looking at it because it lacked concrete horizontal and vertical references for the observer to assess along with the image. The three-dimensional effect produced by the image could not be assessed easily because of the limited size of the image.

The diffuser/two concave mirror combination was more successful as a display because it was comfortable to view. The design took advantage of the three-dimensional imaging that the two mirror system was already capable of generating. This design produced an image that the observer easily perceived as floating above the two mirror system. In essence, the image of the diffuser appearing at the top of the two mirror system acted as the horizontal and vertical reference that was lacking in the previous experiment. The use of depth cues in the image gave the observer the ability to interpret depth.

REAL IMAGING AS A THREE-DIMENSIONAL DISPLAY

I. Introduction

1.1 Background

The human visual system has the innate ability to perceive depth. The mature human visual system is capable of processing a scene in the real world and quickly deciding the relative placement of the objects in that scene. At present, information generated by computers is most commonly displayed on the two dimensions of the computer screen. Humans are capable of processing more information than the two dimensional display can produce. Accurately portraying information to the viewer in three-dimensions would take advantage of the full processing power of the human visual system.

Three-dimensional display technology is in a state of evolution. The advances in this technology over the past few years, however, have produced remarkable results. The ultimate goal of this technology is to display to the viewer a particular scene with such realism in three dimensions that no ambiguity exists in the viewer's mind concerning the depth information in that scene.

Three-dimensional displays operate through a variety of different media and techniques. Some displays use computer graphics for producing three-dimensional

objects on the two-dimensional display. Another technique uses holography to present the proper amplitude and phase of a three-dimensional object to the observer. Still, another technique provides stereoscopic perspective to an observer through special viewing glasses. This technique allows the left and right eye to perceive a slightly different view of an object that together give the observer the information required for depth perception (Wickens, 1990). The list goes on.

When the image source of the 3-D display is a two-dimensional display, the perception of three dimensions relies heavily on the right combination of depth cues as well as the proper display medium. Together, these ingredients create an illusion of depth that the human visual system is accustomed to interpreting in the real world. The illusion can be so remarkable that the observer cannot deny its three-dimensional realism.

1.2 Problem Statement

Three-dimensional representations of objects displayed on a computer screen are currently limited to the bounds of the two-dimensions of the screen. This thesis will use optical elements to project to the viewer as a real image, a computer generated, three-dimensional object. The computer generated object, itself, is generated from the two-dimensional bounds of a computer screen. This thesis will then assess the improvement in three-dimensional realism from this type of display.

1.3 Summary of Current Knowledge

Three-dimensional displays can project an image to an observer with either coherent (laser) or incoherent (ordinary) light. Each type of illumination source has its advantages and disadvantages. The use of coherent light for display purposes is

with few exceptions in conjunction with computer generated holograms. To date computer generated holograms are computationally intense to generate. The benefit of using holograms is that the light coming off the hologram has the same amplitude and phase as the light that would come off of a real object.

The use of incoherent light for the state of the art 3-D displays is more common. These 3-D displays operate either stereoscopically or monoscopically. Stereoscopic displays take advantage of the stereoscopic nature of the human visual system. Stereoscopic vision is a result of the left and right eye perceiving a slightly different view of an object under observation. The slightly different views are then integrated by the viewer's mind. The depth information about that object is then perceived with great accuracy. Monoscopic displays do not take advantage of the stereoscopic nature of the human visual system. They rely mostly on the use of other depth cues to present the viewer an object that can be perceived as having three dimensions.

Many techniques of presenting a three-dimensional scene to the viewer in stereo are in use today. These techniques fall under two categories--stereoscopic and autostereoscopic displays. The difference between these two displays is that autostereoscopic displays do not require the use of special viewing glasses whereas stereoscopic displays do. In order to place a minimum incumbrance on the viewer, the autostereoscopic display is the most desirable display to implement from these two choices.

Many types of monoscopic displays are also in use today. A Silicon Graphics workstation is an example of one type of device that can produce objects with three-

dimensional perspective on a monoscopic, two-dimensional display. This type of display must implement a special technique to portray three-dimensional objects on the two-dimensional computer screen. The technique subjects three-dimensional objects to a data reduction process so that they can be mapped to the computer screen. What this means is that, two of the object's spatial dimensions can be directly mapped to the display screen, but the object's third dimension must be mapped to one or both of two dimensions of the display screen. The mathematics controlling the mapping of the third dimension onto the computer screen has been improved over the years and the three-dimensional image produced on the screen has a striking realism about it. Even so, the mapping of three dimensions on a two-dimensional display screen produces an inaccuracy in the viewer's ability to determine the absolute distance between points in the third dimension. This ambiguity introduced in the process is the shortcoming of this technique.

Another type of monoscopic display uses depth cues in conjunction with real imaging techniques. The display media in this case is a holographic lens. This lens has a short focal length and large area. This display technique has been proven to have a profound effect on the depth perception of the human visual system. By making a monoscopic view of a three dimensional scene, which is generated on a two-dimensional computer screen, float at the top of the lens without any apparent two dimensional bounds, an observer is easily fooled into believing that the scene is three dimensional. This is accomplished even though the second view that normally comes with an autostereoscopic display is missing.

1.4 Assumptions

In order to limit the scope of this project, the following assumptions are necessary. First, the viewer is no closer than 20 cm from the optical display. Second, the eye separation of the viewer is 6.5 cm (Eichenlaub, 1990). Finally, all images generated on the 3-D display are centered on the optic axis of the two concave mirror projector. The optical display being developed in this project will be designed with these assumptions in mind.

1.5 Scope

The scope of this research effort is limited in that the 3-D display being developed will not produce stereoscopic images. The design of the 3-D display will not provide parallax either. The design, however, will be flexible enough where parallax can be added in the future by tracking an observer's head motion and changing the view of the object simultaneously. This will provide horizontal parallax. Past research has shown that vertical parallax is not needed by sitting or standing viewers for accurate perceptions of distance (Kollin, 1989). The 3-D display developed in this thesis will rely solely on the psychophysical illusion of viewing a monoscopic image floating in space.

Although the optical component acting as the three-dimensional display (the two concave mirror projector) is capable of projecting a three-dimensional view over a 360 degree horizontal plane, the 3-D display being developed will have the capability to only project images of an object into a limited field of view in the horizontal plane. This limited field of view does not equal the 360 degree horizontal field of view potential of the two concave mirror projector.

1.6 Approach

This thesis will research the improvement in three-dimensional realism when using optical components to project computer generated three-dimensional objects as real images to the viewer.

The 3-D display will be implemented using two separate methods for comparison in performance and effect. Both methods use the two concave mirror projector. Specific details on the two concave mirror projector can be found in Appendix A and Appendix B. A cross section of the two mirror system is shown in Figure 3.1.

The first method combines the two mirror system with a lens relay to produce a real image above the top hole of the two concave mirror projector. A low intensity, one inch CRT is the source of the computer generated imagery to be displayed by this 3-D display.

The second method combines the two concave mirror projector with a diffuser. The diffuser is placed inside the two mirror system and a high intensity source is used to project an image onto the diffuser. A real image of the image on the diffuser will then appear at the top of the two mirror system.

1.7 Summary

This chapter introduced the benefits of developing a 3-D display. Specifically, a 3-D display takes advantage of the full processing power of the human visual system. As a result, this thesis will develop a 3-D display that projects a monoscopic view of a scene as a real image. Existing devices have shown that a floating image of a scene generated on a two dimensional display does have a compelling three-

dimensional effect. Compared to the coherent display using computer generated holography, which has proven to be computationally intense, this technique promises to perform well as a real time display.

This chapter also provides the assumptions and the scope for this research effort. Chapter II provides additional background information which validates the approach described by this thesis. Chapter III describes the detailed steps required to design and build the 3-D display setups. Chapter IV contains the performance results of the experimental setups. Finally, Chapter V gives a review of the research along with concluding remarks and recommendations.

II. Current Knowledge

2.1 Introduction

Three-dimensional displays are emerging as the next phase in display technology. The sense of depth on a display can be created using different methods. Each method has its advantages and limitations. Whatever type of system is developed to display the three-dimensional view, it is important to make sure that the best combination of different depth cues are used.

Three-dimensional displays offer the viewer a more natural representation of a particular object of interest. It also promises to reduce the tremendous workload that confronts many professionals that have to interpret large quantities of data. For example, the display could lessen the workload for pilots by improving his situational awareness, but a more probable application would be as a C^3I asset for commanders in the field. The risks, however, of implementing the three-dimensional display must be acknowledged during the design of the display. These risks are discussed in this chapter.

Two fundamental methods exist for projecting the three-dimensional perspective to the viewer. One uses coherent light (laser light) and the other uses incoherent light (white light). The advantages and disadvantages of using one or the other will be discussed later in this chapter.

This chapter will discuss the risks that are inherent in trying to develop a three-dimensional display and the different depth perception cues that create the

three-dimensional realism. It will also outline the different technologies currently available to display the three-dimensional scene. This chapter will also include an analysis of the advantages and limitations of these various technologies. The final discussion will focus on why the method chosen as a three-dimensional display for this thesis effort is most likely to perform best.

2.2 Depth Cues and Stereo Perception

The three-dimensional display must accomplish a difficult task. It must present an image that contains depth cues to make the human sense believe that it is looking at a real three-dimensional scene. Ideally, the display system must also take advantage of the major characteristic of the human visual system--stereoscopic perception (Clapp, 1987). Stereoscopic perspective, however, is just another depth cue, and it is not necessarily the strongest. The proper combination of strong depth cues can overcome the lack of a stereoscopic perspective.

The inherent risks when trying to implement the three-dimensional display are that it can produce ambiguous images and reduced precision. The following risks must be considered for the optimum display to be developed.

> 1) Any representation of a 3-D world on a 2-D image surface produces an inherent ambiguity. The absolute distance represented by a point along the line of sight cannot be ascertained with high accuracy, compared to absolute distances parallel with the viewing image plane (the plane orthogonal to the line of sight). (This limitation is also characteristic of direct viewing.) Thus, 3-D displays create the potential for perceptual ambiguity which is not present in a set of orthogonal 2-D displays.
>
> 2) Somewhat related to point 1, the integration of all three dimensions of space into a single 3-dimensional object may result in reduced precision in reading values along any one particular axis[2]. Thus, the improved holistic awareness of space, gained by 3-D representation,

may be gained at the expense of analytic detail.

> 3) 3-D displays usually bring with them an added set of design issues, such as establishing the optimum field of view and viewing angle, along with technological hardware issues (related for example to the need to wear stereoscopic glasses or generate alternating images in stereoscopic displays). . . .
>
> (Wickens, 1990)

Depth cues are the details in an image that humans interpret to make judgements about the relative sizes and locations of different objects in that image. How successful a three-dimensional display is depends on how well these cues are incorporated into the display. The success of the 3-D display being developed in this thesis relies on the use of a combination of the depth cues listed below. These cues are depicted in Figure 2.1, in which the cues depicted are referred to by number below.

> Proximity-luminance covariance: Brighter illumination is generally perceived as being closer to the observer . . .(note the shading on the runway (1)).
>
> Aerial perspective: Greater distances are less clearly defined as if viewed through haze (see the mountains in the upper right (2)).
>
> Shadows: A sense of 3-dimensionality is conveyed by shadows either attached to an object (3) or cast on an adjoining surface (4).
>
> Highlighting: The particular reflection of light off of a curved surface conveys a sense of its 3-dimensionality (see the sphere at the top of the tower to the left of the runway (5)).
>
> Textural gradients are continuous changes in the grain or spatial frequency of texture across the visual field, as shown in the left side of the figure (7). These typically provide cues to the slant of a surface.
>
> Linear perspective describes the cue created by a rectangular surface slanting in depth, which forms two converging lines (see the runway outline (8)).

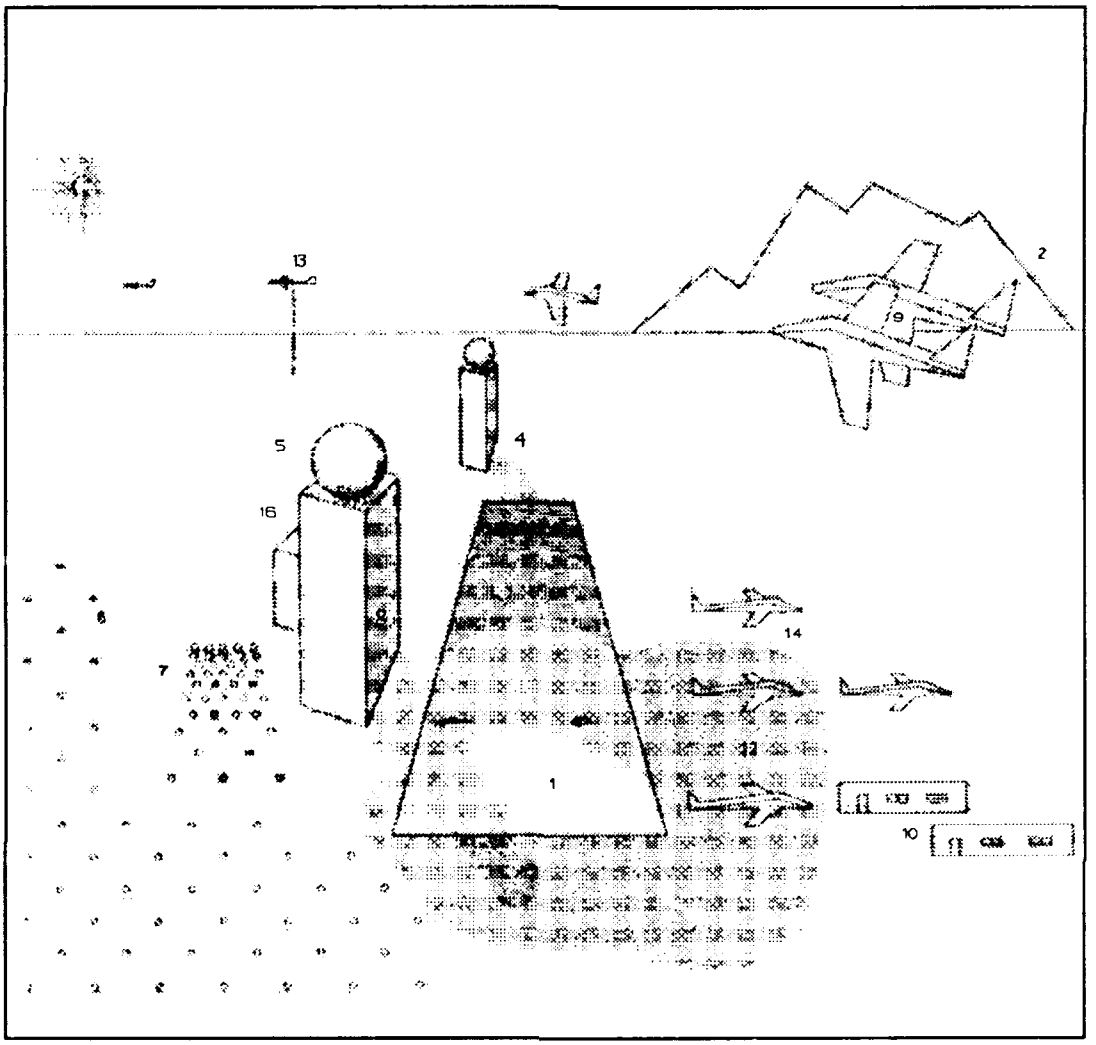

Figure 2.1 Some cues for depth perception.

(Wickens, 1990)

Interposition or occlusion results when the nearer of two objects obscures the contours of the more distant one (see the aircraft in the upper right (9)).

Past experience is used to judge differences in depth. When the observer knows that two objects are of the same true size, then the object casting the larger retinal image is assumed to be closer (compare the two buildings (10), or the three aircraft in the sky (13)).

Height in the visual field is used to judge distance as we view objects situated on a plane below us. Objects that are more distant are then higher in the visual field. Compare the two buildings (10) or the three aircraft sitting on the ground (12 & 14).

> Relative motion may be used as a depth cue in two respects: (i) Rotation of objects conveys a sense of their 3-dimensionality by the changing texture, light, and shadow along the surface of the objects. (ii) Motion parallax defines the relatively greater movement of objects near to the observer as the observer's viewpoint moves perpendicular to the line of sight.
>
> Observer-centered cues refer to the sense of depth conveyed by three properties of the visual system itself (as opposed to the pattern of light reaching the eyes, which is called the retinal image). Accommodation refers to the change in lens shape necessary to bring the image in focus on the back of the retina. Binocular convergence refers to the rotation inward of the two eyes to bring the images of closer objects into alignment on the two retinas. Binocular disparity refers to the disparity in the image cast by the same object, as viewed by the two different eyes. This disparity is conveying depth information for objects that are relatively close to the observer--out to 10 meters or so. However, the cue of binocular disparity, can be exploited through stereoscopic displays to enhance the sense of depth and distance of objects at any distance . . .
>
> (Wickens, 1990)

Not all of these cues must be present to create the three-dimensional perspective. In fact, binocular disparity, motion parallax, and interposition are the predominant cues from which the human sense interprets three-dimensionality (Wickens, 1990).

A three-dimensional display would be most successful if it presented the viewer the two views (one for each eye) that are normally seen in the real world. Accomplishing this takes advantage of the stereoscopic nature of the human visual system. Stereoscopic vision operates only when each eye of the viewer perceives the different views of an object in space. It gives the viewer depth perception, and is an important factor in judgements of motion, size, illumination levels, and scene dynamics and structure (Clapp, 1987). In addition, the following can be said about stereoscopic vision:

> The most important features of stereoscopic vision is that when objects are viewed by both eyes simultaneously, the two images viewed by the eyes merge into one spatial impression. When this stereopsis occurs, the visual field of view is enlarged, and we can see "around the edges" of objects in the visual field. The field of view of one eye extends approximately 150 degrees horizontally and 135 degrees vertically. For both eyes the horizontal field of view is approximately 180 degrees, the overlap of the field of view comprises the stereoscopic field.
>
> (Clapp, 1987)

Using the different depth cues that humans interpret depth from, a display can present an image to the viewer that is similar to what would be seen in the real world.

2.3 Existing Three-Dimensional Display Technology

The current three-dimensional display technology uses either coherent or incoherent optical techniques to project the image to the viewer. The coherent technique uses a laser as the light source. The incoherent technique uses an ordinary light source. Most of the three-dimensional displays used today operate with incoherent light.

Which particular type of illumination is better from the point of view of image spectral content depends very strongly on the detailed structure of the object, and in particular on its phase distribution. Therefore the types of objects to be displayed will dictate the type of illumination that would be best suited (Goodman, 1968). This analysis is very difficult and beyond the scope of this thesis.

2.3.1 The Coherent Approach

The use of holography and the synchronization of a modulated laser beam with a rotating disk are two methods that can be used in a three-dimensional display that uses coherent light.

The use of the holographic technique for a three-dimensional display requires immense computation by a computer. Simply stated, holography is the technique where both the amplitude and phase of an object is recorded (Hariharan, 1984). The amplitude and phase is recorded by interfering the backscatter of laser light coming off an object (the object beam) with the original laser beam (the reference beam) on a photographic plate. When this plate is developed and reilluminated by the same laser, the interference fringes on the hologram produces a wavefront that is identical to the original object beam. To a viewer, the object appears in its original three-dimensional splendor.

To use holography in a real-time three-dimensional display, a computer must predict what the interference pattern from every point on a laser illuminated object is and display it on an optical crystal. The computation of this interference pattern by a computer is more commonly referred to as computer generated holography. When the optical crystal is illuminated by the laser, the laser and the computer generated hologram combine to allow the viewer to see the object with the same three-dimensional realism that an original object would display. A typical four-by-four inch hologram with a 30-degree wide viewing window has about 25 billion bytes of information (Free, 1991). This is a cumbersome number that only a super computer can handle.

The rotating disk approach modulates a low-power laser 10,000 times per second so that it shines points of light on the disk that is rotating at 600 rpm. The beam scans the disk in two dimensions. So as the disk rotates, the two-dimensional image fuses into a three-dimensional image (Campbell, 1990). This type of display

offers a 360° field of view. The image data is sequentially sent to control the laser sweep, and it is repeated every 360 degrees of disk rotation. The image produced by this type of display has a true 3-D volume characteristic.

2.3.2 The Incoherent Approach

Three-dimensional displays that operate with incoherent light rely on using optical elements and/or depth cues to make a three-dimensional image. This type of display does not require the tremendous computation requirements of the coherent computer generated hologram technique.

Incoherent three-dimensional displays fall under two categories--stereoscopic and monoscopic. Stereoscopic displays take advantage of the stereo nature of the human visual system. That is, they present a slightly different view of an object to each eye.

Stereoscopic displays can be described in terms of whether special viewing glasses must be worn. If the glasses are not worn, then the displays are described as auto stereo displays. Stereoscopic displays can also be described in terms of whether the two images are viewed simultaneously or in alternation. These are described as time-parallel and time-multiplexed displays, respectively (Wickens, 1990).

The autostereoscopic display is an ideal type of three-dimensional display since it does not require the viewer to wear cumbersome helmets or glasses. One example of an autostereoscopic display is an computer monitor made by Dimension Technologies. This monitor is made up of a standard liquid crystal display used in combination with a patented backlight illumination system. The backlight has the ability to precisely illuminate the screen such that the left eye sees only the

information displayed on the odd columns and the right eye sees only the information displayed on the even columns. Thus, when a left eye view of some scene is displayed on the odd column pixels and a right eye view is displayed on the even column pixels, the observer will see a stereoscopic image (Eichenlaub, 1990).

The monoscopic display, on the other hand, does not present the two separate views to the observer. This type of display relies heavily on using strong depth cues and optical components to convince the observer that he is looking at a three-dimensional scene. One example of this type of display uses a varifocal mirror. The focal length of the mirror is changed dynamically so as to form a single perspective, three-dimensional image of a cathode ray screen at varying distances above the mirror. The eye then integrates the varying scenes into an apparent volume (Travis, 1990). This can be considered to be a true 3-D display.

The monoscopic display can also be implemented using different types of optical elements to create a real image that is offset from the optic axis of the system. This has been successfully demonstrated using a holographic lens.

The holographic lens transforms an optical wavefront, in much the same manner as an ordinary lens. One of the main advantages of using a holographic lens is that it can be made to be thin, light-weight, and have large apertures (Hariharan, 1984). It can also be made to focus incident rays at a point that is offset from the normal to the surface.

An existing system that uses this holographic lens is a videogame made by SEGA called *TIME TRAVELER*. The system was discovered towards the end of this thesis effort. As a result the holographic lens was not incorporated into this study.

The system, itself, appears to be made up of one holographic lens. An ordinary CRT is used as the source. Figure 2.2 shows the relative placement of the CRT with respect to the holographic lens. It also shows the real image location and orientation to the observer. Notice that the orientation of the image varies with the location of the observer.

The success of the real imaging technique used by this videogame makes the approach for this thesis credible. The videogame projected two-dimensional scenes with three-dimensional perspective. By making these scenes float, an observer perceives a greater three-dimensional effect.

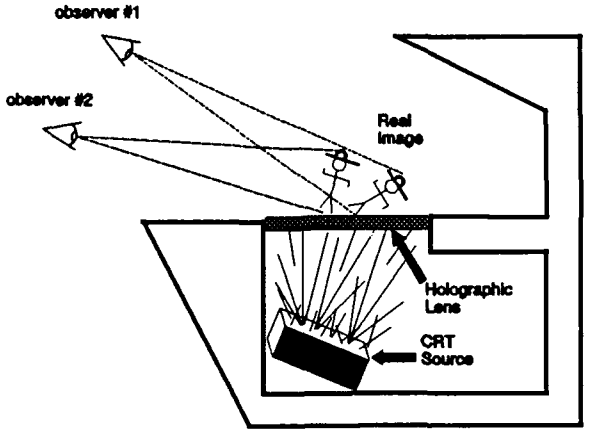

Figure 2.2. Three-dimensional display system using a holographic lens.

2.4 Summary

Three-dimensional displays must represent objects with the proper depth cues so that the human visual system can perceive the three dimensions. The three-dimensional realism will most likely be perceived by the viewer if the predominant depth cues (binocular disparity, motion parallax, and interposition) are used.

A three-dimensional display can be implemented using either coherent or

incoherent light in the display system. The incoherent method is less computationally intensive as the coherent method. Therefore, real-time, three-dimensional displays can be implemented easier using incoherent means. Autostereoscopic displays are the ideal type of three-dimensional display. They offer a more natural view of an object to the viewer. The stereoscopic nature of the display takes advantage of the way the human visual system works. The combination of showing each eye the perspective view of the object and the use of depth cues will give the display an unmistakable three-dimensional effect.

By itself, a monoscopic displays cannot produce images with the same three-dimensional realism as an autostereoscopic display. Using strong depth cues and real imaging techniques, however, the floating, monoscopic view of a scene will have a striking three-dimensional effect to an observer. Another technique that can boost the performance of the monoscopic display tracks the observers head position. This incorporates head motion parallax that is a strong depth cue.

III. Methodology

3.1 Introduction

The approach stated in Chapter I describes the two experimental setups to perform as 3-D displays. The first setup is a combination of a lens relay with the two concave mirror projector. The second setup is a diffuser/two concave mirror projector combination.

This chapter provides specific details on the development of these two experimental setups. The discussion explains the theory behind using the matrix technique to design the lens relay for the first experimental setup. It also explains how the two concave mirror projector works. The optical parameters and field of view limitations of the two concave mirror projector are presented. The 3-D display design for both setups is developed with specific viewing considerations in mind, which are specified in this chapter. The actual setups are discussed in the latter part of this chapter. Finally, a list of required equipment is provided.

3.2 Background

This section gives a brief explanation of the matrix method for analyzing lens relay systems. This method is crucial in simplifying the design of the lens relay for the 3-D display. This section also reveals the optical parameters and field of view limitations of the two concave mirror projector.

3.2.1 Analysis of a Lens Relay Using the Matrix Method

When designing simple optical systems with one or two elements, it is usually

customary to use

$$\frac{1}{s_o} + \frac{1}{s_i} = \frac{1}{f} \tag{3.1}$$

which is known as the gaussian lens formula (Hecht, 1989). The terms s_o, s_i, and f are the object distance from the optical element, image distance from the optical element, and focal length of the optical element, respectively. When the design of the optical system exceeds two elements, the use of this equation can become very tedious. Therefore, the use of a matrix technique becomes extremely helpful.

The matrix technique is simply a series of refraction and transfer matrices that manipulate a ray of light. The refraction matrix describes what happens to a light ray as it passes through an optical element. The transfer matrix describes what happens to a light ray as it propagates between elements. Together, the matrices take a ray that enters the optical system at a known height and angle and give the angle and height of the ray emerging from the system. If the optical elements are assumed to be thin (i.e. they have no thickness), then the refraction matrix is

$$\boldsymbol{R} = \begin{vmatrix} 1 & -\frac{1}{f} \\ 0 & 1 \end{vmatrix} \tag{3.2}$$

where f is the focal length of the optical element, and the transfer matrix is

$$\boldsymbol{T} = \begin{vmatrix} 1 & 0 \\ d & 1 \end{vmatrix} \tag{3.3}$$

where d is the distance separating the optical elements.

The example in Figure 3.1 shows a simple two element optical system that will

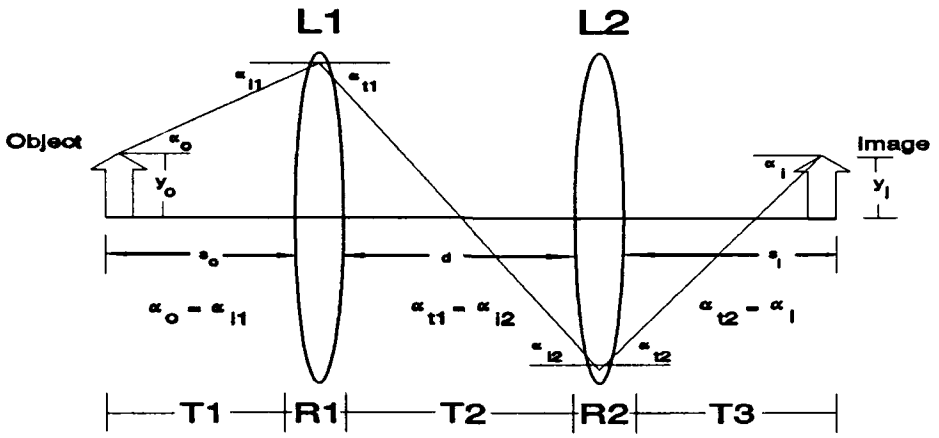

Figure 3.1 A two element example applying the matrix method.

be analyzed using this matrix method. The elements are separated by a distance d, the object distance to the first element is s_o, and the image distance from the second element is s_i. The initial height and angle of the light ray leaving the object is described by y_o and α_o, respectively. The resulting height and angle of the light ray converging at the image is represented by y_i and α_i, respectively, which are the terms to be solved by the matrix method. When y_o and y_i are positive, the ray is above the centerline of the system axis. Likewise, when they are negative, the ray is below the axis. When α_o and α_i are positive, the ray is pointing upward. When they are negative, the ray is pointing downward. The terms T_1, T_2, T_3, R_1,and R_2 represent where the transfer and refraction matrices apply in the figure, and together they form the system matrix. Equation 3.4 solves y_i and α_i for this example.

$$\begin{vmatrix} \alpha_i \\ y_i \end{vmatrix} = \underbrace{\begin{vmatrix} 1 & 0 \\ s_i & 1 \end{vmatrix}}_{T3} \underbrace{\begin{vmatrix} 1 & -\frac{1}{f2} \\ 0 & 1 \end{vmatrix}}_{R2} \underbrace{\begin{vmatrix} 1 & 0 \\ d & 1 \end{vmatrix}}_{T2} \underbrace{\begin{vmatrix} 1 & -\frac{1}{f1} \\ 0 & 1 \end{vmatrix}}_{R1} \underbrace{\begin{vmatrix} 1 & 0 \\ s_o & 1 \end{vmatrix}}_{T1} \begin{vmatrix} \alpha_o \\ y_o \end{vmatrix} \qquad (3.4)$$

3.2.2 *Optical Parameters/Field of View Limitations of the Two Concave Mirror Projector*

The crucial piece of optical hardware that is required to make the 3-D display work is the two concave mirror projector. In order to understand how it performs with other optical elements and how well it performs as a display, an analysis had to be performed.

The analysis set out to find the optical parameters and the field of view limitations of the two concave mirror projector. The specific optical parameters that had to be known were the focal length of the top mirror, f_t, the focal length of the bottom mirror, f_b, and the distance separating the two mirrors, d. The field of view analysis was necessary to assess the performance of the two mirror system as a 3-D display.

The optical parameters were calculated and cross checked using several methods. These methods are described in Appendix A. The results of these methods used in the analysis found f_t=8.2 cm, f_b=7.9 cm, and d=7.8 cm.

The field of view of the two concave mirror projector was quantified using simple geometric techniques. The actual techniques used to derive the field of view equation shown below are described in Appendix B. The results of this analysis found that the field of view is a function of the real image diameter that forms at the top of the two mirror system, *RID*, the distance that the real image forms from the plane of the top hole, s_i, and the inclination angle of the image, β.

The maximum field of view that the 3-D display can provide is 44.9° . Otherwise, the field of view becomes smaller depending on the size of the real

image,its location above the plane of the top hole, and its inclination. The field of view can thus be described by

$$FOV = \tan^{-1}\frac{s_i - RID\cdot\sin(\beta) + 7.5}{RID(\cos(\beta) - 1/2) + 3.4} - \tan^{-1}\frac{s_i}{3.1 - RID/2} \qquad (B.6)$$

where again s_i is the distance that the real image forms from the plane of the top hole, β is the inclination angle of the image, and *RID* is the diameter of the real image that forms at the top of the two mirror system.

3.3 Implementation Methods for the 3-D Display

As briefly discussed in the approach section of Chapter I, the 3-D display will be implemented with two separate experimental setups for comparison in performance and effect. Both experimental setups use the two concave mirror projector shown in Figure 3.2.

The first experimental setup combines the two mirror system with a lens relay to produce a real image above the top hole of the two concave mirror projector. A low intensity, one inch CRT is the source of the computer generated imagery to be displayed by this 3-D display.

The second experimental setup combines the two concave mirror projector with a diffuser. The diffuser is placed inside the two mirror system and a high intensity source is used to project an image onto the diffuser. A real image of the image on the diffuser will then appear at the top of the two mirror system.

This section will describe in detail the two concave mirror projector, the lens relay/two concave mirror projector combination as a 3-D display, and finally the

diffuser in the two concave mirror projector combination as a 3-D display.

3.3.1 The Two Concave Mirror Projector

The primary component in the 3-D display system is a two concave mirror projector. The projector is made up of two concave mirrors that are inward facing. It is approximately 23 cm wide and 8 cm high. A picture of the two mirror system is shown in Figure 3.2. The image of Captain America's head appears at the top hole.

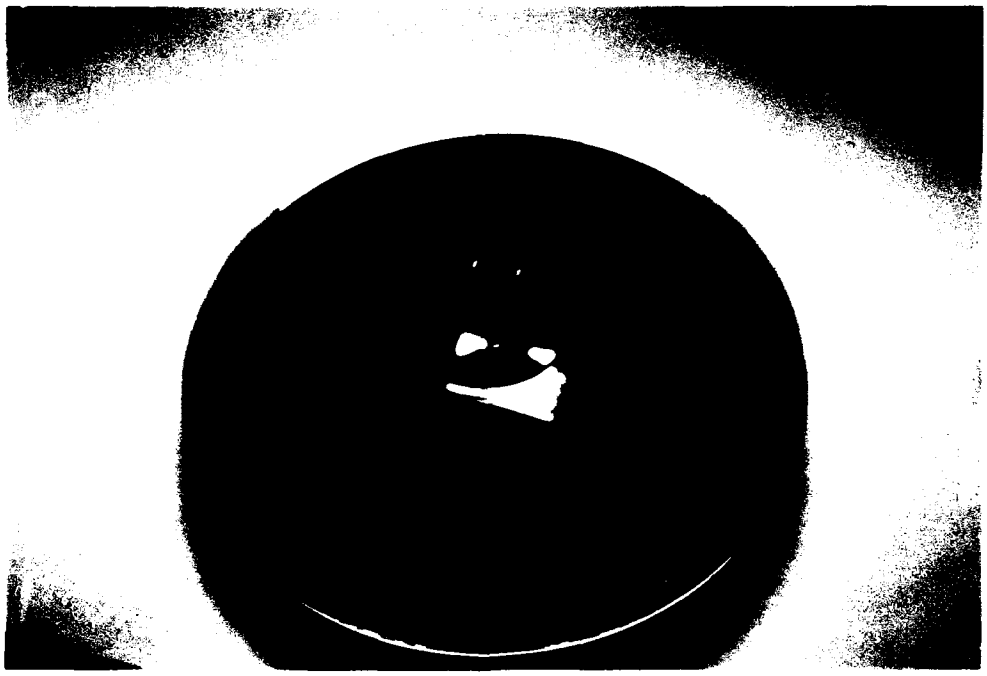

Figure 3.2 A picture of the two concave mirror projector with the image of Captain America's head appearing at the top hole.

A cross section view of the two concave mirror projector is shown in Figure 3.3. This figure also shows how the projector works by itself. The projector works by creating an image of an object placed at the bottom mirror. The image that is created seems to float in space at or above the plane of the hole in the top mirror. If the original object is three dimensional, the resulting image will also be three

somewhere in that field of view with a lens in the background. As a result, an observer will find it difficult to gauge where this real image is located in front of the last lens in the lens system. This lacking depth cue will make a 3-D effect suffer as a result.

The two concave mirror projector, on the other hand, has a field of view that is offset from the center axis. Appendix B explains this field of view characteristic in greater detail. Because the two concave mirror projector can display a real image with an off-axis field of view to the top hole and the fact that the edges of the top hole give a strong reference point for the observer to assess the location of the image, the 3-D effect is enhanced.

The two concave mirror projector has been modified slightly from its original state as depicted in Figure 3.3. A hole has been drilled at the center of the bottom mirror. This hole is approximately the same size as the hole centered on the top mirror. With this new hole in the bottom mirror, computer generated images can be brought into the two mirror system from the bottom.

The addition of this hole to the two mirror system does not affect its performance whatsoever. In Appendix B, the field of view is defined from the edge of the bottom mirror to the point on the bottom mirror where the image of the top hole appears. The diameter of the image of the top hole on the bottom mirror is approximately 6.8 cm. The hole on the bottom mirror is .8 cm smaller in diameter than the image of the top hole on the bottom mirror. Therefore, the new hole does not affect the field of view of the two concave mirror projector.

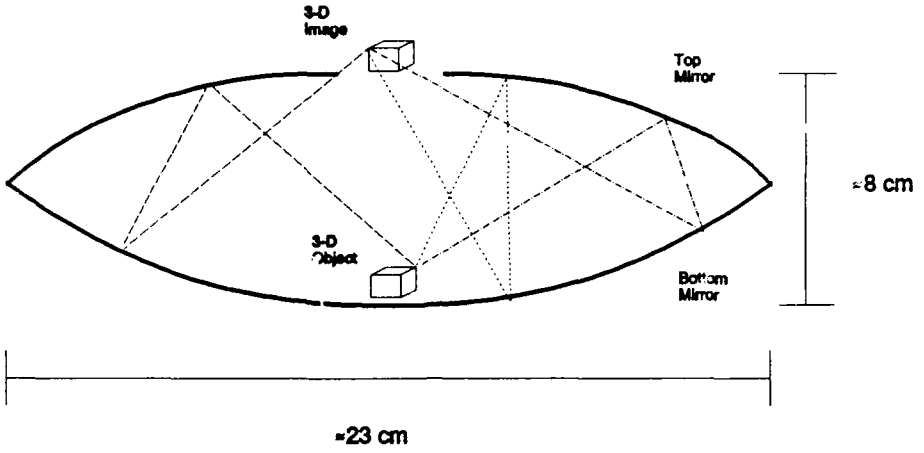

Figure 3.3 A cross section view of the two concave mirror projector. The ray trace showing the image formation is representative of the actual imaging that takes place.

dimensional. In fact, it is very difficult to tell the difference between the image and the real object.

In technical terms, the image that is formed at the top of the projector is a real image. By definition, a real image occurs when an optical element causes the rays coming from an object source to converge at a conjugate point in space. Thus, a luminous image of the object source would appear on a screen placed at this conjugate point (Hecht, 1989). The human visual system will perceive a real image floating in space the same way it would perceive a real object placed in that same location. This makes this two mirror system an ideal candidate for a 3-D display.

The question may arise, why not use a lens system to form the real image of the object instead of using this two concave mirror projector as a 3-D display? A lens system is indeed very capable of performing the same imaging as this two mirror system. The problem with a lens system is that the field of view of this type of system is centered on the optical axis. The real image will appear to float in space

3.3.2 *The Lens Relay/Two Concave Mirror Projector Combination as a 3-D Display Setup*

The first experimental setup to be implemented as a 3-D display consists of the two concave mirror projector in combination with a lens relay system. This combination performs like one optical relay system. An object placed at the beginning of the relay system will emerge at the top of the two mirror system as a real image. In order to take advantage of the 360 degree horizontal field of view of the two concave mirror projector, a typical display could be built according to Figure 3.4.

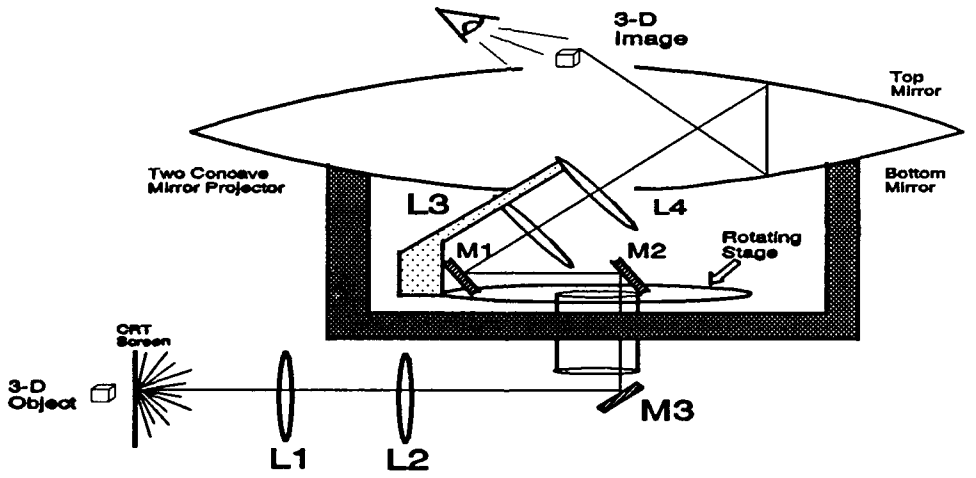

Figure 3.4 A typical 3-D display setup using the lens relay/two concave mirror projector combination. This setup takes advantage of the 360 degree field of view of the two mirror system.

Figure 3.4 shows the two concave mirror projector receiving images from a lens relay system built on a rotating platform. The rotating platform is necessary to allow the 3-D images to be projected from the two concave mirror projector at any angle in the possible 360 degree horizontal field of view.

Before any 3-D system like the one shown in Figure 3.4 can be built, the experimental setup must first be proven on an optics bench. The experimental setup

will line up the lens relay with the two concave mirror projector to perform the imaging depicted in Figure 3.4. The only difference is that the image will only emerge from the two mirror system in one horizontal direction with a finite field of view in the vertical and horizontal direction. This limited field of view in the horizontal direction justifies the development of the second experimental setup, described in the following section, in which the field of view is large in the horizontal direction.

3.3.3 Diffuser/Two Concave Mirror Projector Combination as a 3-D Display

The second experimental setup to be implemented as a 3-D display places a diffuser inside the cavity of the two concave mirror projector. A high intensity source illuminates the diffuser with an image.

The diffuser, itself, is placed in the two mirror cavity so that it is imaged at the top of the two mirror system very much like the object that is imaged in Figure 3.3. When the diffuser is illuminated by the photon source projecting a scene, the scene will also appear to float at the top of the two mirror system.

A typical display using this combination could look very much like the display shown in Figure 3.4. The only difference is that the lens relay must be set up to focus an image onto the diffuser placed at the bottom of the two mirror cavity.

3.4 Design of the 3-D Display

The two experimental setups introduced earlier, the lens relay/two concave mirror projector combination and the diffuser/two concave mirror projector combination, are designed in this section.

The design process takes into account the required viewing considerations for

both types of display. It then uses the matrix method to calculate the required separation distances for the lenses in the lens relay, and it uses the gaussian lens formula to find the required separation of the object source and lens for performing simple imaging on the diffuser.

3.4.1 Viewing Considerations

Two viewing considerations have to be addressed when designing the 3-D display. The first is that the display must project the image at the lowest possible angle to the horizontal plane of the top hole of the system. This viewing consideration is the objective for both display combinations.

The lowest possible viewing angle is found from the analysis in Appendix B of the field of view limitations of the two concave mirror projector, and is called $\theta 1_{min}$. From Appendix B, $\theta 1_{min}$=24.2°. It is the belief that by allowing the observer to see the image from this angle and by simultaneously making the inclination angle of the image, β, as large as possible, the image will appear to stand up at the surface of the top hole. This is a crucial component to giving the viewer the perception that the image is floating above the two mirror system. The combination of this floating image with the appropriate depth cues in the image should create a compelling 3-D effect.

The second viewing consideration only applies to the lens relay/two concave mirror projector combination and it addresses comfort. If the optical relay is not set up with comfortable viewing in mind, the viewer will find himself straining to overcome an accommodation/convergence conflict. This conflict and the criteria for comfortable viewing is described in Appendix C. The comfort equation that is

derived in Appendix C is restated below.

$$x = \frac{si\,(ES + RID)}{FOVT \cdot D_{AS} - RID} \qquad (C.2)$$

where *RID* is the desired real image diameter, *FOVT* is the desired field of view tolerance, D_{AS} is the diameter of the aperture stop of the optical relay, s_i is the desired image location from the top of the display, and *ES* is the eye separation of the viewer. Together these variables find x, the minimum distance that the viewer can be from the image location without experiencing discomfort.

3.4.2 Lens Relay Design Using the Matrix Method

The lens relay that will be used in the lens relay/two concave mirror projector combination is designed using the matrix method described earlier. The use of this matrix technique along with three specific design guidelines provides the specific relay setup required for the display.

The first of the three guidelines is to design the relay from the image plane to the object plane. In essence, design the relay backwards. This gives control over the size and location of the real image. The comfort criteria must be considered to help decide what the image size and location should be.

The second guideline is to model the two concave mirror projector as a two lens system as shown in Figure 3.5. This will help simplify the ray trace through the two mirror system.

Finally, the third guideline is to ensure that the top hole of the two concave mirror projector is the aperture stop of the relay system. The reason for this is that the 3-D display will perform better if the viewer can't see the finite size of the other

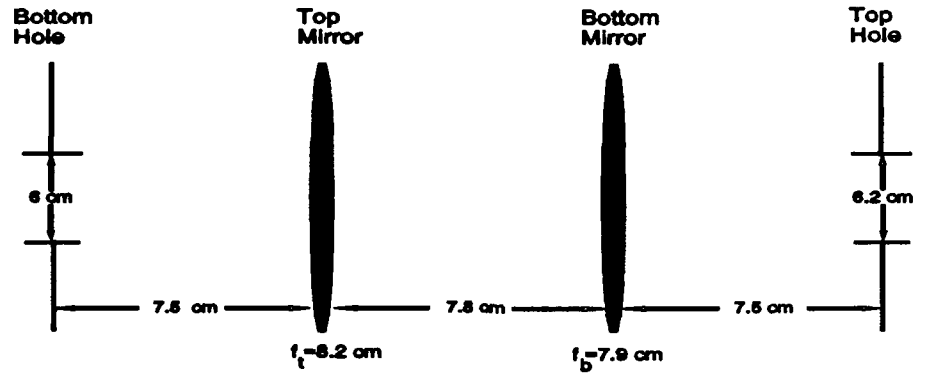

Figure 3.5 Modelling the two concave mirror projector as a two lens system.

optics in the relay. The matrix method can easily be used to uphold this guideline.

At this point in the design, a danger exists that the chosen size and location for the real image could force the half diameter of the bottom mirror of the two concave mirror projector to be the aperture stop of the system. The reason that only half of the bottom mirror is viewable to the observer is due to the angled display nature of the projector.

To determine which of the two apertures is the aperture stop, the two angles, $\theta 1_{min}$ and α_i, must be compared. The angle, $\theta 1_{min}$, is derived in Appendix B and describes the minimum field of view angle achievable by the two mirror system. The angle, α_i, is defined in Appendix E and it is the angle of the ray coming from the image to the edge of the top hole of the two mirror system. This angle is similar in concept to the angle, α_i, shown in Figure 3.1. If α_i is greater than $\theta 1_{min}$ then the half diameter of the bottom mirror is the aperture stop, otherwise the top hole of the two mirror system is the aperture stop.

The typical design of the optical relay system is shown in Figure 3.6. Because the focal lengths of the two mirrors are so short and the variety of lenses available

is limited, four lenses are required to fulfill these design guidelines.

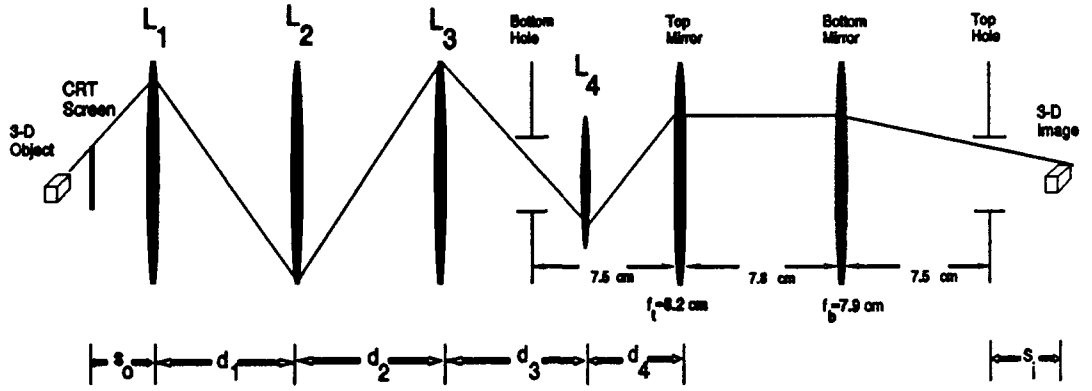

Figure 3.6 Typical design of the lens relay/two concave mirror projector 3-D display combination.

The design of the relay begins with the declaration of all known parameters. These include:

1. The focal length and diameter of all optical elements.

2. The field of view tolerance, *FOVT*, the eye separation of the viewer (the average eye separation is 6.5 cm), *ES*, and the diameter of the top hole, D_T

3. The desired image location, s_i, image diameter, *RID*, and inclination angle, β.

4. The object diameter, *OD*.

The goal of this analysis is to make sure that the light rays coming from the source make it through the entire optical relay. To ensure that the light rays do not stray from the relay, they must be monitored at six different locations. These locations can be seen in Figure 3.6. Starting from the image, each location, which is better thought of as a subsystem, encompasses a propagation distance and one optical element. In essence, the matrix technique will analyze each subsystem, which is

comprised of one refraction and one transfer matrix, separately.

Combining the refraction and transfer matrices yields a subsystem matrix that has the general form

$$A(d,f) = \begin{vmatrix} 1-\frac{d}{f} & -\frac{1}{f} \\ d & 1 \end{vmatrix} \qquad (3.5)$$

where d and f are the distance that the light ray travels in that subrelay system and the focal length of the optical element in that subrelay system, respectively.

The separation between optical elements must be chosen not only to keep the light rays from the object within the relay but also to ensure that the top hole in the two concave mirror projector is the aperture stop of the relay system. Fulfilling these two requirements requires parallel analysis of two unique ray traces. The first trace simulates what the viewer would see if his eye was located at the image plane of the optical relay. The second trace simulates what the viewer would see if he were located at a point in the far field from the display. These two rays will follow different paths through the optical relay.

The viewer will be located anywhere between the far field and the image location with respect to the display. These two traces, therefore, represent the boundary conditions to be used in this matrix method to ensure that the top hole is the aperture stop of the system.

Recall that the matrix technique yields information concerning the height and angle of a light ray emerging from an optical system. Since the goal of using this technique is to calculate the required separation of all optical elements, except the

fixed separation distance between the two mirrors in the two concave mirror projector, a conversion equation is required.

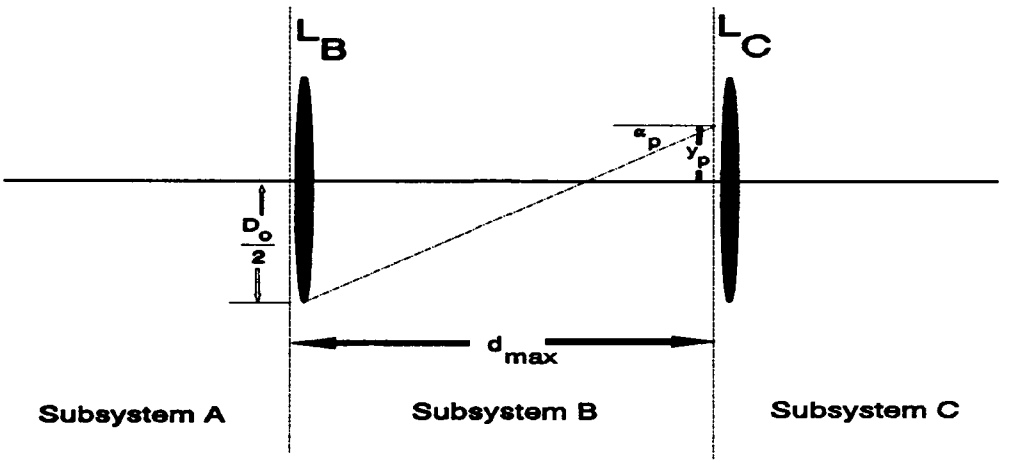

Figure 3.7 Depiction of the ray parameters and how they govern the maximum separation between optical elements in a lens relay.

The maximum distance that the optical element in a subsystem can be from the optical element of the previous subsystem occurs when the light ray of interest coming from the previous optical element hits the edge of the subsequent optical element. This is depicted in Figure 3.7. Using this rule of thumb, the conversion equation that will find the maximum separation distance between the optical elements, d_{max}, can be written as

$$d_{max} = \frac{\frac{D_o}{2} - y_p}{\alpha_p} \qquad (3.6)$$

where D_o is the diameter of the optical element the light ray is currently in, y_p is the height of the light ray emerging from the previous optical element, and α_p is the angle of the light ray emerging from the previous optical. The angle term, α_p, is always small for the size optics being used, which allows for the simplified equation. This

conversion equation must be applied to the two unique ray traces separately. The numerical results can then be compared. Since the design must make sure that both light rays stay within the relay boundaries, the smallest value for d_{max} between the two unique rays must be chosen as the maximum separation distance allowed.

Once the maximum separation distance between all optical elements have been found, an iteration technique is required to find the actual separation distances required to perform the desired imaging. This is done by propagating two rays that originate from the same point on the image through the optical relay. Where these two rays emerge and intersect is the required object location.

The MATHCAD file SYSTEM4.MCD performs the two trace analysis described earlier and performs the iteration technique described above. A hardcopy of this file can be found in Appendix E. The numerical calculations appearing on the hardcopy represent the actual setup that was used in the 3-D display.

3.4.3 Imaging on the Diffuser Using the Gaussian Lens Formula

The gaussian lens formula is defined in equation 3.1. It gives the relationship between the object and image location and the focal length of the optic.

The diffuser/two concave mirror projector combination is simplistic in design compared to the lens relay/two concave mirror combination. Only one lens is required to image the object onto the diffuser. The object is generated on an LCTV screen. The dimensions of the screen are 6 cm x 4.5 cm. The average object diameter on this screen is 2.54 cm x 2.54 cm. Since the dimensions of the diffuser are approximately the same as the size of the object, the required magnification of this one lens imaging system is 1. Since the magnification for a one lens system is the

ratio of the image distance to the object distance, this design calls for an image distance, s_i, that is equal to the object distance, s_o. This can only happen when both of these distances are equal to $2f$ (two times the focal length of the lens). Therefore, the rule of thumb for this design depends on the focal length of the lens being used. The object and image distance will be twice the focal length of the lens.

3.4.4 The 3-D Display Designs

This section proposes the two experimental display designs that will be setup to assess their performance as 3-D displays.

The first experimental setup, the lens relay/two concave mirror projector combination, is shown in Figure 3.8. Using the design MATHCAD file,

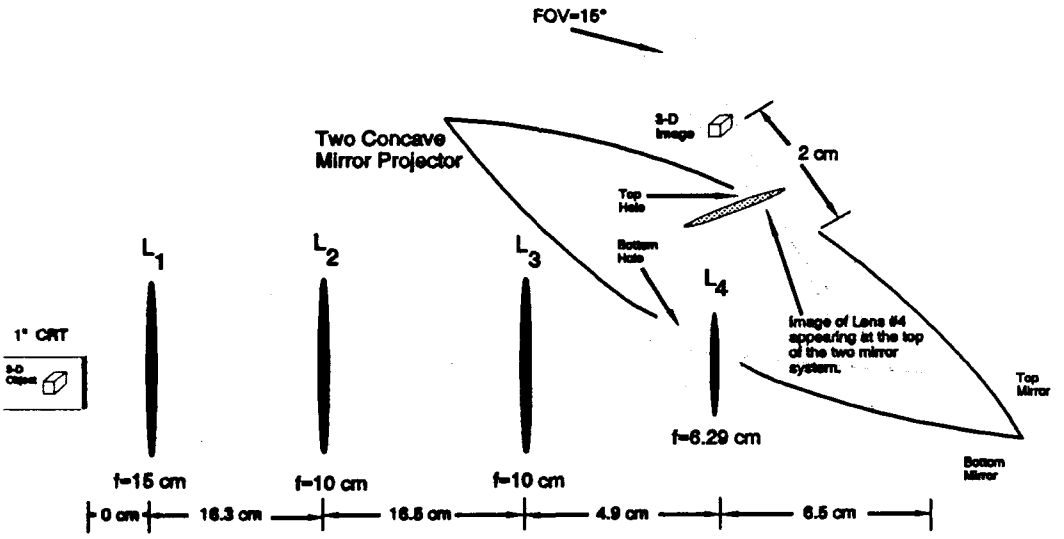

Figure 3.8 The proposed lens relay/two concave mirror projector experimental setup.

SYSTEM4.MCD, the following performance parameters are easily calculated: The setup produces an image that is 2.54 cm in diameter and is located 2 cm from the top hole of the two mirror system; The minimum observer viewing distance is 20.7 cm;

The expected field of view is limited by the two mirror system to 15 degrees given that the inclination angle of the image as measured from the horizontal is approximately 45 degrees.

The second experimental setup, the diffuser/two concave mirror projector combination, is shown in Figure 3.9. The lens used in this setup is an achromat with a focal length of 30 cm. The diffuser is placed 6.75 cm from the top mirror and

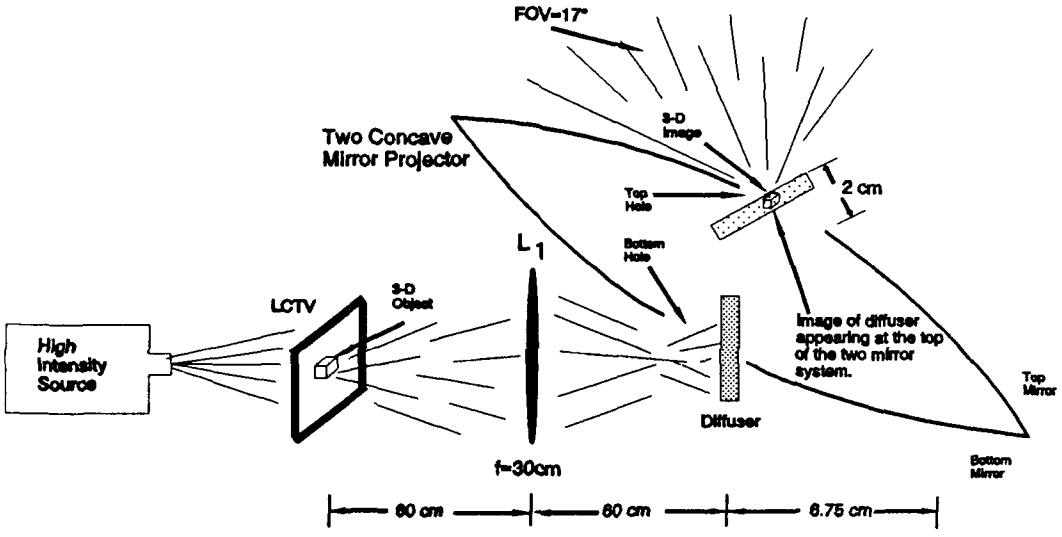

Figure 3.9 The diffuser/two concave mirror projector experimental setup.

therefore its resulting image forms 2 cm from the top hole of the two mirror system. The size of the image on the diffuser is 2.54 cm x 2.54 cm. This in turn is imaged at the top hole of the two mirror system with the dimensions 3.05 cm x 3.05 cm as a result of the 1.2 magnification introduced by the two mirror system. This image location and magnification is calculated by the MATHCAD file TCMP.MCD located in Appendix E. The field of view is limited by the field of view of the two concave mirror projector since the diffuser now acts like a real object. The field of view is

calculated using equation B.6 derived in Appendix B. The inclination angle of the diffuser in the two concave mirror projector is approximately 60 degrees from the horizontal. Therefore, the expected field of view, which is calculated by TCMP.MCD, is 17 degrees.

3.5 Equipment Required

This research effort required the use of software and hardware resources. The Silicon Graphics Iris 4D workstations were used to produce the three dimensional computer generated objects that will be the input to the optical relay. In addition, several demo programs existed to produce different three-dimensional simulations on the workstation.

The Silicon Graphics workstation had to interface with a controller that drove three monochrome one inch CRTs. The green CRT was used as the object source for the lens relay/two concave mirror projector setup. The green CRT was chosen because the human eye responds to this color the best.

An LCTV was used to act as an input to the diffuser/two concave mirror projector setup. The LCTV was slightly modified so that a high intensity light source could illuminate it from the back side. The image of the object on the LCTV could then be focused on the diffuser.

The remaining materials required for this thesis effort fell under the category of optical components. The two concave mirror system was the primary optical component required. Other components such as lenses, irises, and mirrors were required as needed.

Additional specific information concerning the use of these resources can be

found in Appendix D.

3.6 Validation of the Methods Used To Implement the 3-D Display

The two experimental setups shown in Figures 3.8 and 3.9 both take advantage of the illusion that the two concave mirror projector is capable of generating.

As originally presented in Figure 3.3, the two concave mirror projector produces a real image of a real object placed at the bottom of the two mirror system. If a two dimensional view of a three dimensional object is generated on a computer screen and this in turn is imaged at the top of the two mirror system, the illusion of the image floating above the top hole should improve the observer's evaluation of the object's three dimensionality.

3.7 Summary

The two experimental 3-D display setups are shown in Figures 3.8 and 3.9. The displays rely on the illusion creating capability of the two concave mirror projector. A 6 cm hole added to the bottom of the projector so that images can be brought in through the bottom does not hurt the field of view of the two mirror system.

The two designs project their images into a finite field of view. At this point, the three-dimensional realism of this one directional image is important. Future improvements to the design (i.e. adding a rotating platform at the bottom) could take advantage of the 360 degree horizontal field of view of the two mirror system.

The design of these setups requires the disclosure of the optical parameters and field of view limitations of the two mirror system, specific viewing considerations, and a matrix analysis. The design of the lens relay/two concave mirror combination

setup required the development of a specific design method using the matrix analysis. The relay has to be analyzed in separate sections to ensure that the light rays of interest stay within the relay.

The success of these designs relies heavily on the floating illusion that the two concave mirror projector is already capable of producing. As a result, the inclination angle of the image, β, is very important. As this angle gets larger, the image at the top of the two mirror system appears to stand up, and the perception of a floating image is enhanced. The negative effect of making this angle very large is that the field of view suffers.

Finally, a list of the required equipment to implement both display setups is provided.

IV. Results and Analysis

4.1 Introduction

This chapter describes the results obtained when the two experimental setups shown in Figures 3.8 and 3.9 were implemented. The analysis of the results is subjective. It explains the observer's perception of the floating image generated by both setups.

4.2 Results

4.2.1 The Lens Relay/Two Concave Mirror Projector Combination

The lens relay/two concave mirror projector combination fell short of its expected performance as a three-dimensional display.

Several lens combinations were used, in addition to the lens combination proposed in Chapter 3, to generate real images of different sizes and at different locations above the top hole of the two mirror system. The creation of these different images was necessary to assess the effect on the observer's perception. Using a piece of white paper as a screen, the size and location of the various images were verified against their expected values. During this verification, small adjustments from the theoretical separation distance between the optical elements were made to compensate for the slight deviation from the ideal values of the lens focal lengths.

The two concave mirror projector was oriented in many different ways to change the inclination angle, β, of the image appearing at the top. The three-

dimensional realism of the real image was subjectively assessed at the different angles.

The different orientations effectively caused the image to emerge from the two mirror system at an angle ranging from $\theta 2_{max}=70.1°$ to $\theta 1_{min}=24.2°$ measured from the horizontal. These angles were derived in Appendix B to describe the field of view limitations of the two concave mirror projector. At an orientation angle at or around $\theta 2_{max}$ the location of the real image was harder to perceive than when the image was at or around $\theta 1_{min}$. Even at an angle near $\theta 1_{min}$, the image location was still not easy to gauge.

The lens relay/two concave mirror projector setup proposed in Figure 3.8 had to be slightly modified to optimize the size and location of the real image. The modified experimental setup used is shown in Figure 4.1. A picture of the actual setup is shown in Figure 4.2.

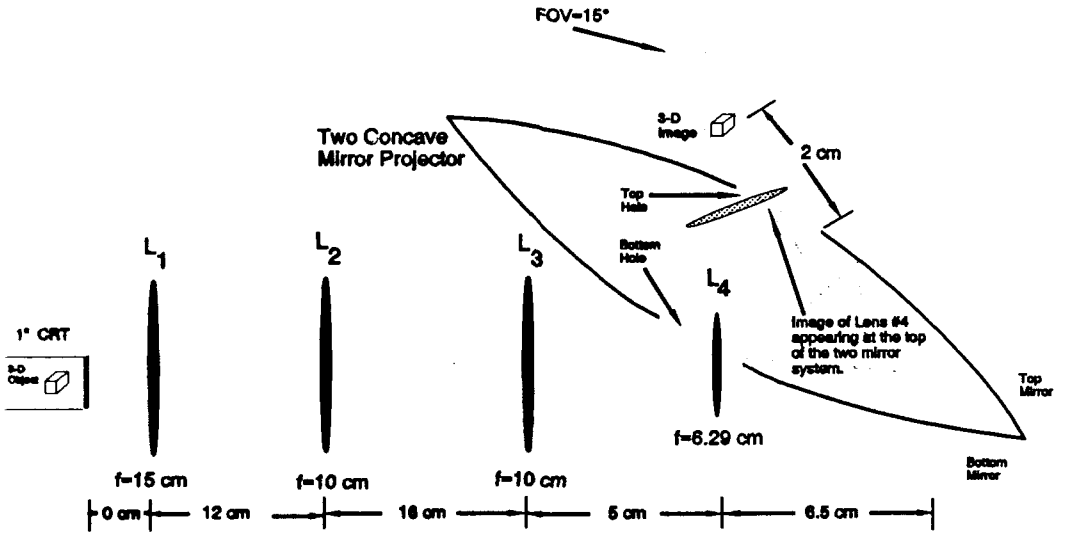

Figure 4.1 The actual lens relay/two concave mirror projector experimental setup used.

as an observer views the display. As you can see, no compelling sense that the image is floating 2 cm above the system exists. The image, however, does appear to be located somewhere just inside the two mirror cavity, showing that an observer can view a real image.

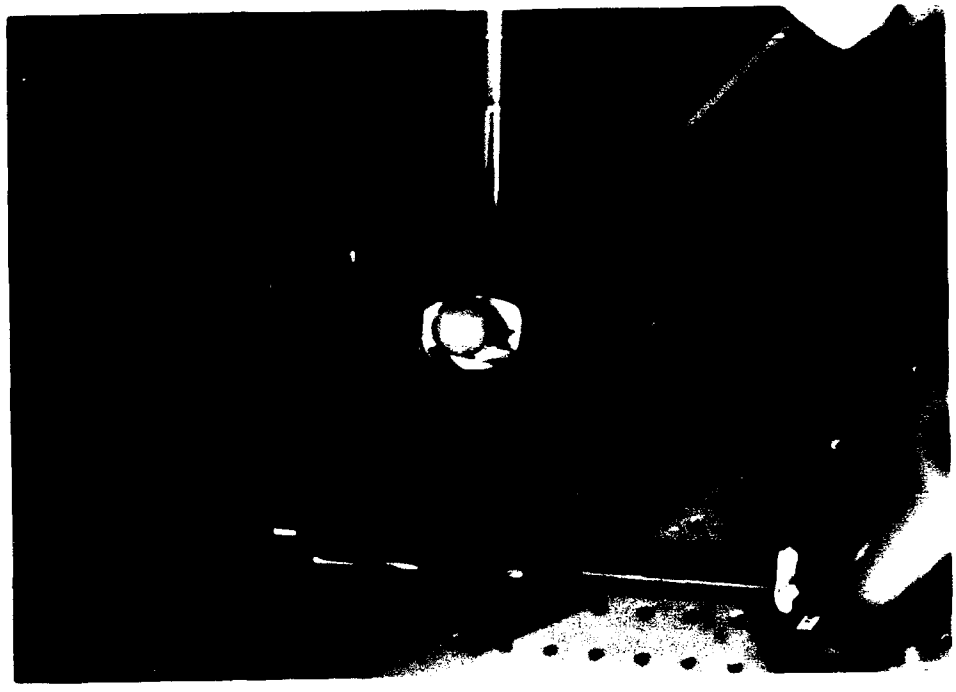

Figure 4.3 Photograph of the real image formed at the top of the two concave mirror projector by the lens relay/two concave mirror projector experimental setup.

The location of the real image could be gauged if the observer tried to touch the image. The relative placement of the observer's finger with the image was a strong depth cue that led the observer to realize the location of the real image. If the observer's finger obscured the image, the image would appear to be pushed back into the two concave mirror projector cavity.

Figure 4.4 shows an observer's finger placed relative to the position of the same real image shown in Figure 4.3. The observer's finger is obscuring the edge of

This setup produced an image with a diameter, *RID*, of 2.54 cm at a distance, s_i, of 2 cm from the top of the two mirror system. The angle of the two concave mirror projector with respect to the field of view axis of the lens relay was approximately 45 degrees as originally proposed in Chapter 3.

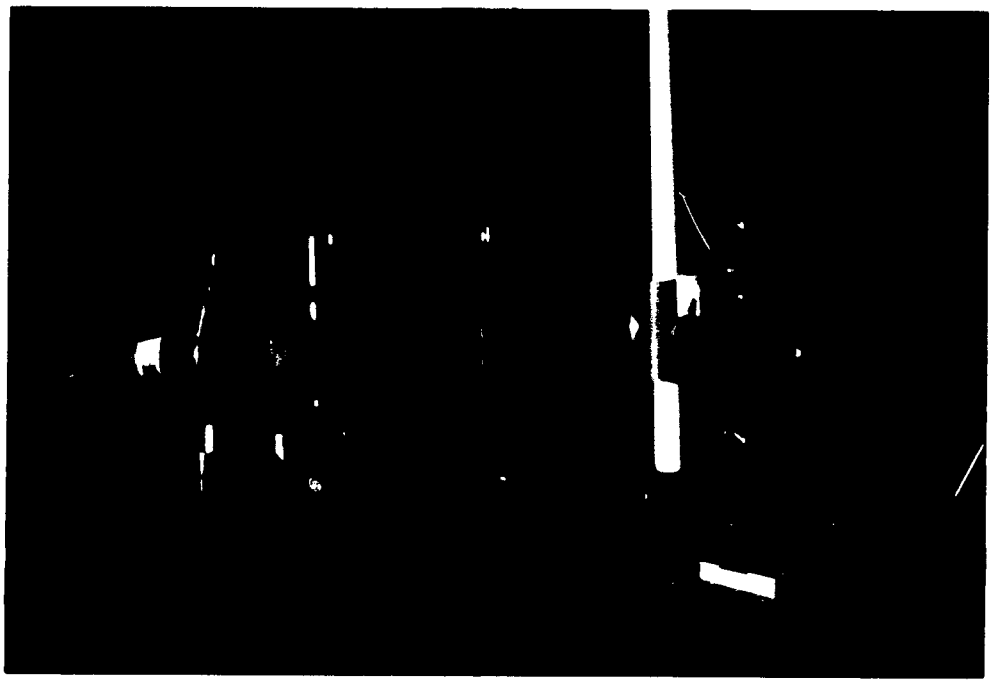

Figure 4.2 A picture of the actual setup used to test the lens relay/two concave mirror projector combination as a 3-D display.

Although the real image generated formed above the top hole of the two mirror system, it did not appear to float there with the same effect as the image of a Captain America's head as depicted in Figure 3.2. This was true for the different observers who looked at the real image. One could tell that the real image was forming somewhere in front of the bottom mirror of the two concave mirror projector, but it never seemed to escape the top hole of the two mirror system.

Figure 4.3 shows a photograph of a real image that was formed by the experimental setup shown in Figure 4.1. The picture is taken from the same angle

the image slightly so the image does not seem to be next to the finger. Also, the camera could not capture the binocular effect that an observer possesses. For this reason, the placement of the finger next to the image is more compelling when observed directly than when it is observed in a picture.

Figure 4.4 The real image formed by the lens relay/two concave mirror projector with an observer's finger placed relative to the image location.

Another problem encountered with the image was that this setup caused a slight strain on the observer's eyes. The cause of this strain was explained in Appendix C as an accommodation/convergence conflict. This conflict was severe when other lens combinations were tried. It was so severe, in fact, that the image would appear to split to the observer as his left and right eye relaxed. The degree of accommodation/convergence conflict was reduced substantially when the observer moved away from the display. The drawback was that the detail in the image was

difficult to ascertain from this distance. The size and location of the image in the setup shown in Figure 4.1 was such that the observer could be relatively close, ≈20 cm, to pick out the details in the image and not have the image split.

The size of the image seemed to be critical in whether the image was perceived as being outside or inside the two concave mirror projector. During the design of the lens relay, the image size and location was a controllable quantity. If the size of the image was made to be larger than the aperture stop, or in this case the top hole of the two mirror system, the image would not project itself above the two mirror system regardless of whether the observer tried to touch it or not.

The quality of the image was not without its flaws. The short focal lengths of the two mirrors and three of the four lenses caused a slight distortion of the image. The distortion would get worse if the separation of the lenses was increased. The system, also, did not perform well for multi-color images because the lenses used were not achromats. They introduced chromatic aberrations. The setup shown in Figure 4.1 shows that a single color CRT was used as an input to the system to negate this aberrant effect.

The lens relay/two concave mirror projector combination performed best when the lights in the room were off. The reason for this was that the one inch CRT was not a strong photon generator. Details in the image could best be seen when the lights were out. Another reason was that the background lights would cause multiple reflections on all the optical surfaces. These surfaces would be imaged through the relay and would give the illusion that the image was floating behind a piece of glass that was somewhere inside the two mirror cavity. This defeated the goal of making

Figure 4.6 Image of the diffuser when the photon source is off. Notice that the image appears to be coming out of the two mirror system.

Since the diffuser radiated light into a wide angle, the image formed at the top of the two concave mirror projector possessed similar qualities to an image of a real object that diffuses light from the bottom of the two mirror system. The expected field of view for the image formed by this experimental setup was 17 degrees. The actual field of view was measured to be approximately that.

This experimental setup did not produce the accommodation/convergence conflict that the previous experimental setup seemed to have a problem with. It seems that the image was easier to view when it was radiating outward into a wide field of view from a diffuser.

When the photon source for this experimental setup was off, the image of the diffuser was clearly seen at the top of the two mirror system as seen in Figure 4.6.

an image appear to float in space.

4.2.2 The Diffuser/Two Concave Mirror Projector Combination

The diffuser/two concave mirror projector combination produced a much different result than the lens relay/two mirror system combination. The diffuser/two concave mirror projector combination seemed to take advantage of the "mystical" imaging that is performed by the two mirror system by itself. Again, this imaging is shown in Figure 3.2.

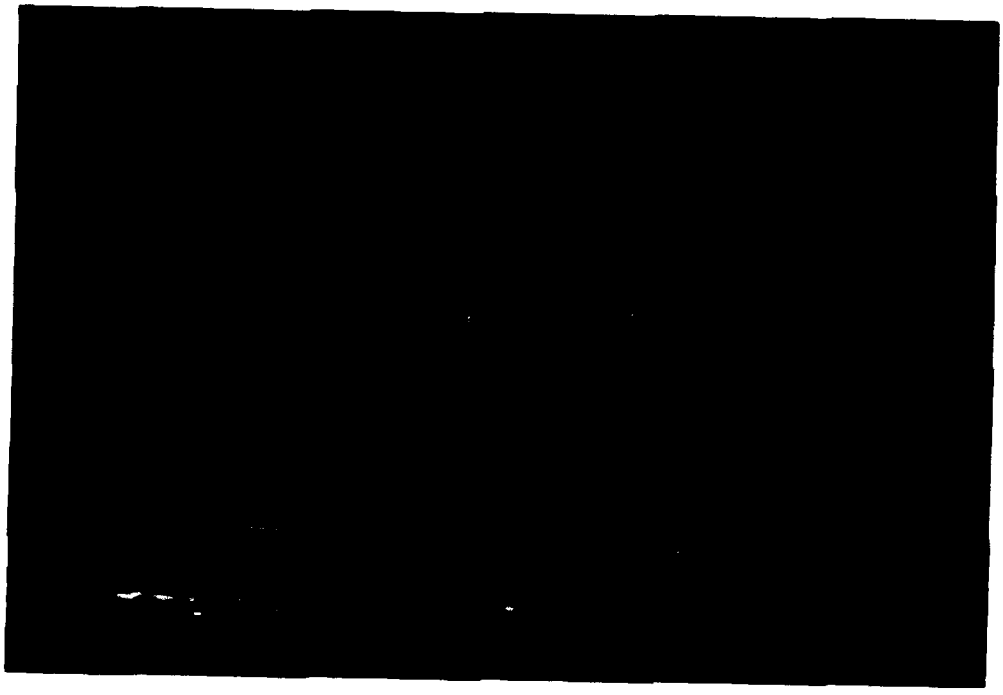

Figure 4.5 A picture of the actual setup used in the test of the diffuser/two concave mirror projector combination as a 3-D display.

The design for this experimental setup was increasingly simpler than the setup for the lens relay combination. The experimental setup shown in Figure 3.9 did not have to be modified to improve its performance. Since this setup only used one lens, the alignment of the object and diffuser was not difficult. A picture of the actual setup used is shown in Figure 4.5.

Figure 4.7 Image formed by the diffuser/two concave mirror projector experimental setup.

The image of the diffuser is forming about 2 cm from the top of the two mirror system. The diffuser made a nice mask to hide the optics from the observer. Thus there were no distractions in view to the observer to take away from the floating effect of the image.

When the photon source was on, the intensity of the image focused on the diffuser was very high. The result was that the diffuser seemed to become transparent and the image was the only perceptible feature from this display. The image can be clearly seen in Figure 4.7.

This experimental setup was also very nice in that it was not photon limited like the lens relay/two concave mirror projector experimental setup. The lights in the room could be kept on. The observer had plenty of light coming from the image. In fact, so much light was coming from the image that the room lights didn't affect

the fidelity of the floating image in an adverse manner.

4.3 Analysis

4.3.1 The Lens Relay/Two Concave Mirror Projector Combination

The results obtained for this experimental setup revealed several interesting facts. For this setup the inclination angle of the image had a noticeable effect on how the observer perceived the image. If the image was made to stand up relative to the plane of the top hole, the illusion of the image floating was improved. The improvement unfortunately was not significant enough to make the image seem to float above the top hole.

The results also revealed that the placement of real objects around the image (in this case the observer's finger was used) helped tremendously in gauging where the image location was. In fact, this turned out to be a compelling depth cue for this type of display. Since the real image was floating with no relative screen nearby, it was extremely difficult for the observer to tell where the image was located. This type of display would require real objects to be placed near the image to help the observer gauge where the image was forming. The objects would act as relative vertical planes for the image floating at the top. If a relative horizontal plane could be added, the observer would perceive the location of the image with even greater accuracy.

The fact that the two concave mirror projector was used as the 3-D display limited the potential size of the real image that could form at the top. If a large image was desired so that the details in the image could be easy to pick out, the field of view would suffer. In addition, the comfort criteria dictated that the allowable

distance that the image could form from the bottom mirror had to get smaller. On the other hand, if a small image was chosen, the field of view would be larger and the image location could be farther from the bottom mirror. The only drawback was that the detail in the image would be very difficult to pick out. In a 3-D display where picking out subtle depth cues is so important, this becomes an unforgivable restriction. A larger scale version of the two concave mirror projector would alleviate this tradeoff.

As a 3-D display, this setup suffered in that the image had little detail due to its limited size. The image location was very difficult to ascertain. The favorable characteristic of this design was that it had a controllable field of view in the vertical and horizontal direction. If the design in Figure 3.4 were implemented using this lens relay approach, discrete views of an object could be displayed at the top of the two mirror system as the rotating stage revolved. In theory, if the rotating stage could revolve fast enough and if the different views of the object could be generated fast enough on the computer, a 3-D perspective of an object would appear over the entire 360 degree horizontal field of view. The observer would, as a result, experience horizontal parallax which would enhance the 3-D realism.

4.3.2 The Diffuser/Two Concave Mirror Projector Combination

The results obtained for this experimental setup revealed similar facts to those stated for the previous setup. The inclination angle of the image in this setup had just as big an impact as it had in the previous setup. If the image was made to stand up relative to the plane of the top hole, the image actually appeared to escape the confines of the two mirror system. It was easy to perceive this because the diffuser,

which itself is a 3-D object, was imaged at the top of the two mirror system just like any other 3-D object would be imaged. When the images from the LCTV were focused on the diffuser, the images naturally appeared to float along with the diffuser.

This setup had a much larger field of view in the horizontal plane than the previous setup. This made viewing the image alot easier. The diffuser projected the image into a 360 degree horizontal field of view.

This setup possessed the advantage of 3-D realism that the previous setup was lacking. The diffuser acted as relative object with respect to the image. This was something that the observer could pick up on immediately. The only unfortunate limitation of this setup was that if a one wanted to implement a rotating stage architecture as depicted in Figure 3.4 to take advantage of the 360 degree horizontal field of view of the two mirror system, it would not work well. This of course is due to the large horizontal field of view of the image introduced by the diffuser.

4.4 Summary

The two experimental setups proved that a real image of an object could be imaged at the top of the two concave mirror projector. Overall, the results indicate that out of the two 3-D display experimental setups tested, the diffuser/two concave mirror projector seems to offer a better image to the observer.

The diffuser/two concave mirror projector combination produced an image that filled a large field of view. This allowed the observer to have some freedom to move his head without loosing portions of the image. This was a big problem with the lens relay/two concave mirror projector combination. Since it had a narrow field of view, the observer would easily loose the image if his head strayed too far from the

center of projection.

If the rotating stage design shown in Figure 3.4 was going to be implemented, the finite size of the field of view produced by the lens relay/two concave mirror projector combination would be best for displaying discrete views of a 3-D object As the stage would rotate, the discrete views would fuse into an apparent stereogram. This architecture would take full advantage of the 360 degree horizontal field of view of the two concave mirror projector.

V. Conclusions and Recommendations

5.1 Introduction

This chapter gives a brief summary of the research performed by this thesis. The conclusions derived from the results of this research are then described. Lastly, recommendations for further research are provided.

5.2 Summary

This thesis effort evaluated the performance of two experimental setups as 3-D displays.

The first setup was made up of a lens relay/two concave mirror projector combination. A low intensity, one inch CRT was used as an input to the lens relay. An image of the 3-D scene displayed on the CRT was successfully formed at the top of the two concave mirror projector. The drawback to this success was that the image was difficult to view. The image location was not easily gauged. Only when the observer tried to touch the image did the location become apparent. The perceived image location was important because it was a key effect that helped the observer believe what he was seeing. This belief was a key factor in perceiving the illusion that was required for the 3-D effect.

Another problem with the image was that an observer felt a slight discomfort while viewing it. This discomfort was a result of a accommodation/convergence conflict. It was difficult for the observer to position his head within the narrow field of view of the image. This made it difficult for both eyes to receive their respective

view of the image. The slight deviation of the observer's head from the field of view of the image resulted in the observer's eyes having to converge on the image to accommodate for the missing pieces of the image.

The low intensity output of the CRTs limited the performance of this setup. The best performance from this setup was observed when the room lights were turned off. With the room lights off, the multiple reflections off of all the optical surfaces were reduced considerably, which helped the image appear as if it were floating by itself.

The diffuser/two concave mirror projector experimental setup used a high intensity source to project images from an LCTV onto a diffuser placed at the bottom of the two concave mirror projector. The diffuser, itself, was imaged at the top of the two mirror system like any other object that is placed at the bottom would be imaged. As with any other object placed at the bottom of the two mirror system, the illusion at the top of the two mirror system was dramatic. It was very easy for the observer to perceive. There was no eye strain and no confusion regarding its location and depth. The results using the diffuser produced a great effect and were by far better results than the first experiment.

When the photon source was on, the image focused on the diffuser would appear to float above the two mirror system. The wide dispersion of light from the diffuser took advantage of the maximum field of view offered by the two concave mirror projector.

Another benefit of using the diffuser was that it blocked the optics that preceded it to the observer. This got rid of a great deal of peripheral distraction with

the image. It was very difficult to design the four lens relay in the previous experimental setup to meet this same condition. The lack of peripheral distraction gave the image floating at the top of the two mirror system a bigger boost.

5.3 Conclusions

The use of real images to project a computer generated object to a point in space requires some additional components in order to create a compelling effect. The lack of vertical and horizontal reference planes in the first experiment made it very difficult for the observer to gauge where the image was formed. These missing reference planes were present in the second experiment. The image of the diffuser at the top acted as the two reference planes.

The two experimental 3-D displays tested in this thesis each had its own strengths and limitations. Out of the two, however, the diffuser/two concave mirror projector performed the best as an autonomous display.

This display did not cause viewing discomfort to the observer. The diffuser dispersed the light in a way that took advantage of the field of view of the two concave mirror projector. The only draw back was that the diffuser reduced the clarity of the image.

This display also took advantage of the observer's perception. By making an image float with an apparent screen created by the diffuser, the observer was easily fooled into believing that the image was floating above the two mirror system.

The use of real images as a display medium produced encouraging results. The most significant conclusion to this research is that a 3-D display can work even when the display doesn't map out a true volume. The human factors side of

producing a 3-D display has a tremendous input. Using the proper optics and depth cues, the observer can be led to believe what he is seeing is three dimensional.

5.4 Recommendations

The lens relay/two concave mirror projector combination produced a real image that had a very narrow field of view. Although this presented a problem for viewing, this design has the potential of becoming a stereoscopic display. If the lens could be oscillated between two positions fast enough to present a left and right view to the observer without flicker, then this design would work very nicely as an autostereoscopic display.

The diffuser/two concave mirror projector combination would work well as a 3-D display if the observers head motion could be tracked so that as he moved around the two mirror system, the perspective of the scene would change accordingly. Although this type of display would not provide the binocular disparity that the human visual system expects, it would provide horizontal parallax to the display.

Future research in this area would be better accomplished with the use of the holographic lens introduced in Chapter 2. The lens adds several benefits that were lacking in this thesis by using the two concave mirror projector. One benefit is that the holographic lens can be made to be very large. If a 20 inch CRT is used as a source for images in a setup using a holographic lens, the lens could easily be manufactured to be that large also. Matching the size of the lens to the source allows a large proportion of the source energy to be focused by the lens.

Another benefit of using a holographic lens is that the focal length can be made to be very small and the optic axis where the rays are focused can be made to

be offset from the normal. Recall that for comfortable viewing the real image is best perceived if it is close to the lens. The off-axis orientation of the focused image creates a sense of depth. The image appears to stand up on the lens surface.

With a short focal length/offset optic axis and a large diameter, the holographic lens can easily produce real images that appear to stand up on the lens surface and the large diameter allows for a large field of view.

Appendix A. The Two Concave Mirror Projector Optical Parameters

This appendix discusses how the optical parameters of the two concave mirror projector (i.e., the focal length of the top and bottom mirror and the distance separating them) were derived, and how the two concave mirror projector works.

The optical parameters of the two concave mirror projector, or the Mirage as it is known commercially, were not available from the manufacturing source--Opti-Gone Associates, Van Nuys CA, (818) 988-1500. The Mirage was designed and built 14 years ago. The tooling for the machinery that makes this device has not been changed since then. The actual specification sheets describing the dimensions of the two mirrors and their separation are lost. The only clue that the manufacturing source could give me was that the two mirrors are not truly parabolic they are spherical. These mirrors can exhibit any one of a range of many degrees of sphericalness. They can range from slightly parabolic to extremely spherical. As a result, the mathematical analysis used to find the focal lengths of the two mirrors and their separation had to be derived using careful physical measurements and taking into account that the mirrors could either be parabolic or spherical.

The two concave mirror projector is made up of, as the name implies, two concave mirrors. The two mirrors face each other and are separated by a distance d. Each mirror has a hole at its center. The projector is usually held in an upright orientation where one mirror is on top of the other. Therefore, the top mirror has a designated focal length f_t and the bottom mirror has a designated focal length f_b.

The derivation of these focal lengths and the separation distance was done by placing the two concave mirrors in two separate x,y cartesian coordinate system plots (Figure A.1). Several independent measurements showed the top mirror width to be 22.6 cm and the bottom mirror width to be 22.2 cm. The height of each mirror was measured by placing the mirrors face down against a flat surface and measuring how far the edge of the holes centered on each mirror was from the flat surface. In both cases, the height of each mirror was 3.6 cm. The diameter of the hole in the top mirror was 6.2 cm and the diameter of the hole in the bottom mirror was 6 cm.

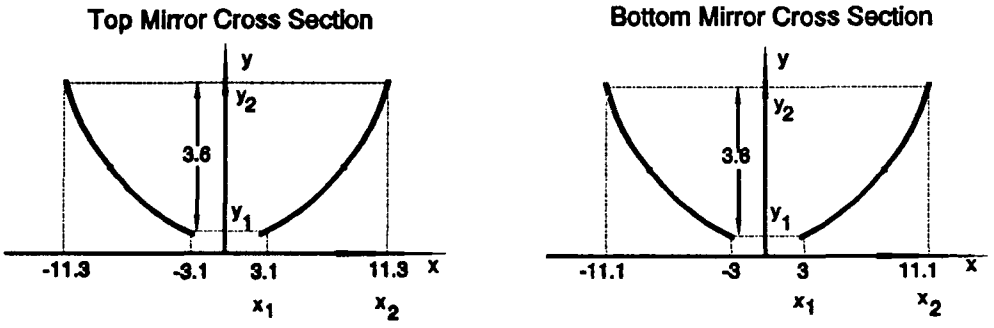

Figure A.1 The cross section of the top and bottom mirrors of the two concave mirror projector. This shows the physical measurements that were taken to help find the optical parameters.

Mathematically speaking, these concave mirrors can be approximated by two parabolas with a slight deviation that makes them spherical. Let P_t and S_t describe the parabolic and spherical shape of the top mirror, respectively. Likewise, let P_b and S_b describe the parabolic and spherical shape of the bottom mirror, respectively. P_t and P_b are described in equation A.1. S_t and S_b are just P_t and P_b, respectively, with a deviation term added which is described by equation A.2.

$$P_t = \frac{x^2}{4f_t}$$

$$P_b = \frac{x^2}{4f_b} \qquad \text{(A.1)}$$

The deviation term, δx, is described as a sum over n,

$$\delta x = \sum_{n=1}^{m} \frac{x^{2n+2}}{2^{n+1}\,(n+1)!\,(f/2)^{2n+1}} \qquad \text{(A.2)}$$

for m=1,...,N where N is an integer. The larger the value of m the more spherical the mirror becomes. The term f is the unknown focal length of the top or bottom mirror. Therefore, S_t and S_b can be written as

$$S_t = P_t + \delta x$$

$$S_b = P_b + \delta x \qquad \text{(A.3)}$$

Notice, however, that the equation for the deviation, δx, at n=0 is identical to the equation for the parabola in equation A.1. Therefore, equation A.4 can be simply stated as

$$S_t = \sum_{n=0}^{m} \frac{x^{2n+2}}{2^{n+1}\,(n+1)!\,(f_t/2)^{2n+1}}$$

$$S_b = \sum_{n=0}^{m} \frac{x^{2n+2}}{2^{n+1}\,(n+1)!\,(f_b/2)^{2n+1}} \qquad \text{(A.4)}$$

for m=0,1,...,N where N is an integer.

To find the focal length of each mirror take the equation for the parabolic or

spherical mirror and use the x values taken from the physical measurements shown in Figure A.1. The y-axis to the edge of the hole, x_1, the y-axis to the edge of the mirror, x_2, and the corresponding difference in their y values, $y_2-y_1=3.6$, can be used in these equations to solve for the focal lengths.

Once these focal lengths have been found, the distance separating the mirrors can be calculated by using the x value corresponding to the edge of the top and bottom mirror in the appropriate parabolic or spherical equation to find the corresponding y value. By adding the y value of the bottom mirror with the y value of the top mirror, the total separation distance becomes apparent.

The MATHCAD file OPTIPARM.MCD performs the numerical analysis described above to find the focal lengths of each mirror and the distance separating them for two cases. A hardcopy of this file is located in Appendix E.

At this point, it is obvious that there are two key variables which affect the outcome of what is calculated for the focal lengths of the mirror and the separation distance. The first is to decide whether to treat the mirrors as parabolic or spherical. The second is to change the spherical degree factor, n. Table A.I shows the numerical results using this MATHCAD file over a range and taking into account these two key variables. For n=0, the analysis is treating the mirrors as parabolic. For n=1,2,...,25, the analysis is treating the mirrors as spherical.

The results shown in Table A.I point out that the spherical degree, n, does not have nearly the same effect as the difference between treating the mirrors as spherical or as parabolic in shape. For n=0 (parabolic case), the focal length of the top mirror, the focal length of the bottom mirror, and the distance separating the two

Table A.I The calculated focal lengths for the top and bottom mirror for the parabolic and spherical case.

n	Focal Length of Top Mirror	Focal Length of Bottom Mirror	Separation Distance
0	8.200	7.900	7.800
1	36.230	35.125	7.250
2	36.414	35.311	7.723
3	36.424	35.320	7.723
4	36.422	35.320	7.723
5	36.420	35.320	7.723
10	36.423	35.321	7.723
15	36.424	35.318	7.723
20	36.424	35.318	7.723
25	36.424	35.318	7.723

mirrors was calculated to be 8.2 cm, 7.9 cm, and 7.8 cm, respectively. For n=1,2,...,25 (spherical case), the average focal length of the top mirror, the average focal length of the bottom mirror, and the distance separating the two mirrors was calculated to be 36.42 cm, 35.32 cm, and 7.72 cm, respectively. The results for the calculated separation distance was equivalent for both cases. The results for the focal lengths of the top and bottom mirror, however, were drastically different, and only one could be correct.

To find which set of the calculated focal lengths best fit reality, two methods of validation were used. The first method of validation tested each mirror separately. The second method of validation tested the two mirrors in their usual inward facing configuration.

Figure A.2 shows the setup that was used to test each mirror individually. An object slide was placed in front of a HeNe laser at different distances from the fixed mirror, s_o. For each s_o position the resulting image distance, s_i, would be found by

translating a screen along the path of the reflecting light until a focused image of the object was obtained.

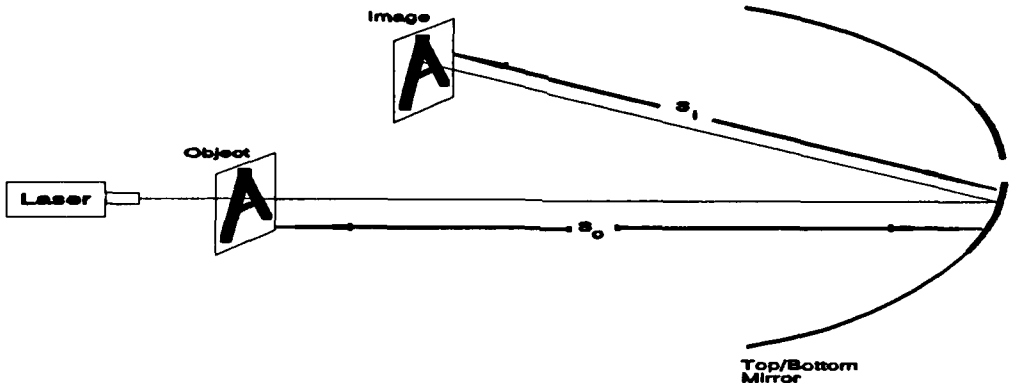

Figure A.2 Validation technique used to verify the focal lengths of the top and bottom mirror.

After recording several object and image positions, the average focal length for the top and bottom mirror was found, using equation A.5 below, to be 8.2 cm. This quantity is *consistent* with the set of parameters that were calculated assuming that the concave mirrors were parabolic.

$$f = \frac{s_o\, s_i}{s_o + s_i} \qquad (A.5)$$

The second method of validation can best ce understood by gaining an understanding of how the two concave mirror projector works. The two mirror system can be modelled as a two lens system separated by a distance d. The bottom hole is separated from the top mirror, and the top hole is separated from the bottom mirror by the same distance d minus δd_b and δd_t, respectively. The model of the projector is shown in Figure A.3.

The deviation terms δd_b and δd_t describe the distance that the edge of the hole in the bottom and top mirror, respectively, is from the apex of the respective

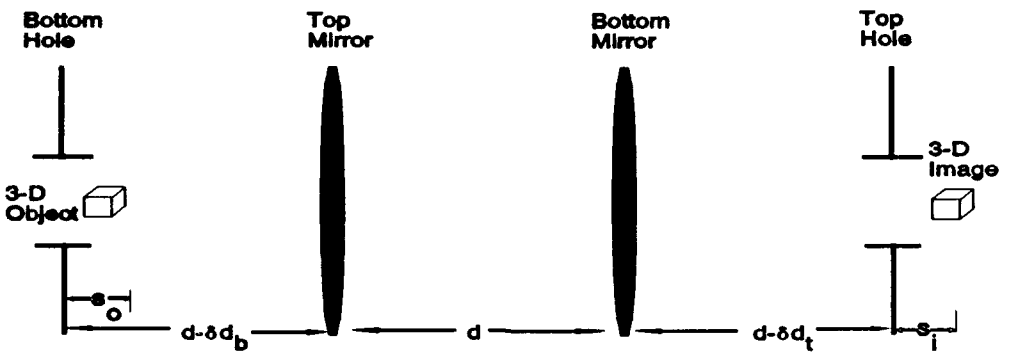

Figure A.3 Generic lens model of the two concave mirror projector.

mirrors. This can be seen in Figure A.1. Notice that the edge of the holes of both mirrors are offset from the axis by y_1. The term y_1 and the deviation terms, δd_b and δd_t, describe the same physical quantity. Now that the focal lengths of the mirrors have been narrowed down to two choices, the numerical value for these deviation terms can be directly calculated by using equation A.4. For the top mirror, use $x=3.1$ *cm* and $f_t=8.2$ *cm* for the parabolic case, and use $x=3.1$ *cm* and $f_t=36.42$ *cm* for the spherical case. For the bottom mirror, use $x=3$ *cm* and $f_b=7.9$ *cm* for the parabolic case, and use $x=3$ *cm* and $f_b=35.32$ *cm* for the spherical case. The result is $\delta d_t=.29$ *cm* and $\delta d_b=.29$ *cm* for the parabolic case, $\delta d_t=.07$ *cm* and $\delta d_b=.06$ *cm* for the spherical case.

According to the rules of optics, any object that is placed in front of the first lens in Figure A.3 will be imaged by the second lens. The relative position of the image with respect to the second lens, s_{i2}, can be found at

$$s_{i2} = \frac{f_2 d - f_2 s_{o1} f_1/(s_{o1} - f_1)}{d - f_2 - s_{o1} f_1/(s_{o1} - f_1)} \qquad (A.6)$$

where s_{o1}, f_1, f_2, and d are the object distance from the first lens, the focal length of

the first lens, the focal length of the second lens, and the distance separating the lenses, respectively (Hecht, 1989).

According to Hecht, once the location of the image, s_{i2}, is found, the magnification, M_T, of the resulting image will be

$$M_T = \frac{f_1 s_{i2}}{d(s_{o1} - f_1) - s_{o1} f_1} \qquad (A.7)$$

Equations A.6 and A.7 can easily be put in terms of the model shown in Figure A.3. If a 3-D object is placed a relative distance from the plane of the bottom hole, s_o, then the distance that the image forms from the top hole, s_i, can be described by equation A.8 below.

$$s_i = \frac{d\cdot(f_b - A) + f_b\cdot A + \frac{B\cdot(f_t\cdot A - f_t\cdot f_b)}{B - f_t}}{d - f_b - \frac{f_t\cdot B}{B - f_t}} \qquad (A.8)$$

where

$$A = d - \delta d_t$$
$$B = d - \delta d_b - s_o$$

Using the image location result, s_i, from equation A.8, the resulting magnification of this image is

$$M_T = \frac{f_t\cdot(s_i + d + \delta d_t)}{d\cdot(s_o - f_t) - s_o\cdot f_t} \qquad (A.9)$$

Both sets of calculated parameters can now be placed in equation A.8 and A.9 above to see which set best fit the way the projector operates. The object distance, s_o, is assumed to be at the plane of the bottom hole. Using the set of parameters

derived for the parabolic case, s_i is calculated to be .5 cm and M_T is calculated to be -1.018. On the other hand, using the set of parameters derived for the spherical case s_i is calculated to be -42 cm and M_T is calculated to be 2.5. The former result means that the image forms .5 cm above the top hole and is the same size but a flipped version of the object, while the latter result means that the image forms -42 cm below the top hole and is 2.5 times larger than the object.

A quick test will show that placing an object at the plane of the bottom hole will cause an image to form somewhere at the top hole that is a flipped version of the object. It is very difficult to tell where the image is formed exactly, but the fact that the image forms at the top hole and it is roughly the same size but flipped version of the object, and not -42 cm below the top hole and roughly 2 times greater in size than the object gives the second validation to treat the concave mirrors as parabolic during mathematical analysis.

In summary, it appears that mathematically the mirrors can be approximated parabolically. After using two methods of validation on the calculated optical parameters, the focal length of the top mirror, the focal length of the bottom mirror, and the distance separating the two mirrors were found to be approximately 8.2 cm, 7.9 cm, and 7.8 cm, respectively.

The two concave mirror projector operates just like the two lens system shown in Figure A.3. Given an object location from the first lens, the location and magnification of the image can be easily calculated using equation A.8 and A.9, respectively. The MATHCAD file, TCMP.MCD, uses these two equations to model the two mirror system. A hardcopy of this file is located in Appendix E.

Appendix B. Field of View Limitations of the Two Concave Mirror Projector

This appendix explains the limitations in the field of view of the two concave mirror projector. The analysis assumes that the object placed at the bottom of the two mirror system is radiating light in all directions. For the case of the lens relay/two concave mirror projector combination described in Chapter 3, the field of view will be determined more by all the optics involved and not just by the two concave mirror projector. The field of view of the two concave mirror projector will, however, always be a limiting factor.

This analysis, therefore, applies more to the diffuser/two concave mirror projector combination described in Chapter 3, since the diffuser radiates into a wide angle that uses the field of view potential of the two mirror system. In the process of calculating the field of view relation, this analysis will show which parameters directly affect the field of view.

The physical dimensions of the two concave mirror projector are outlined in Appendix A. In short, the two mirrors are approximately 23 cm in diameter, and each one has a 6 cm hole centered on it.

The holes create a dead zone that is centered on the optic axis of the two mirror system. If the viewer strays into this dead zone, the real image at the top of the two concave mirror projector will appear to vanish.

The field of view of the two mirror system is offset from this dead zone.

Figure B.1 shows the physical boundaries that make up the field of view. For an object that is radiating in all directions, the viewer can move around the two mirror system and see the real image floating at the top over the entire 360 degree horizontal plane as long as he stays within the field of view.

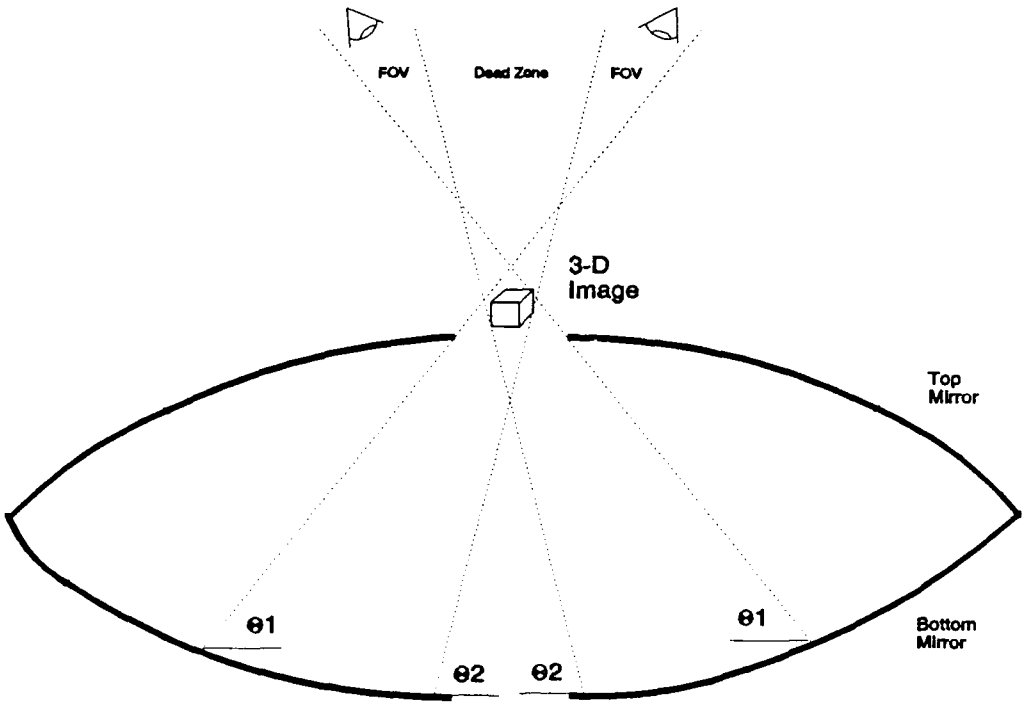

Figure B.1 The physical boundaries of the two concave mirror projector that limit the field of view. For an object that radiates in all directions inside the two mirror system, the field of view shown is revolved about the center axis.

The figure shows that the field of view is a dynamic quantity. It can change its size depending on the size and location of the real image that is formed at the top of the system. Figures B.2 through B.6 show the geometry for each angle term of interest.

From Figure B.2, it is apparent that $\theta 1_{min}$ is a fixed angle which is formed

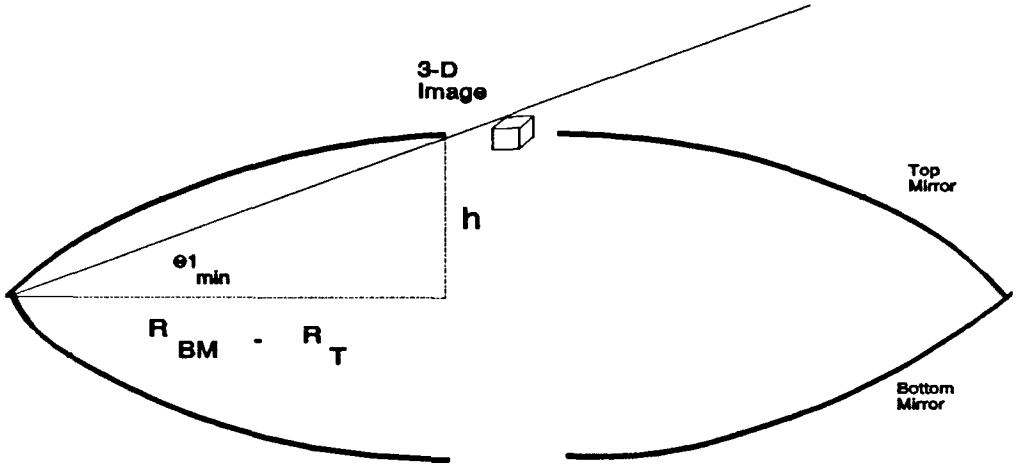

Figure B.2 Graphical explanation of the angle term $\Theta 1_{min}$.

from the edge of the bottom mirror to the edge of the hole in the top mirror. Its equation and numerical value are shown in equation B.1 where the quantities R_{BM}, the radius of the bottom mirror, R_T, the radius of the hole in the top mirror, and h, the height of the top mirror are known to be 11.1 cm, 3.1 cm, and 3.6 cm, respectively.

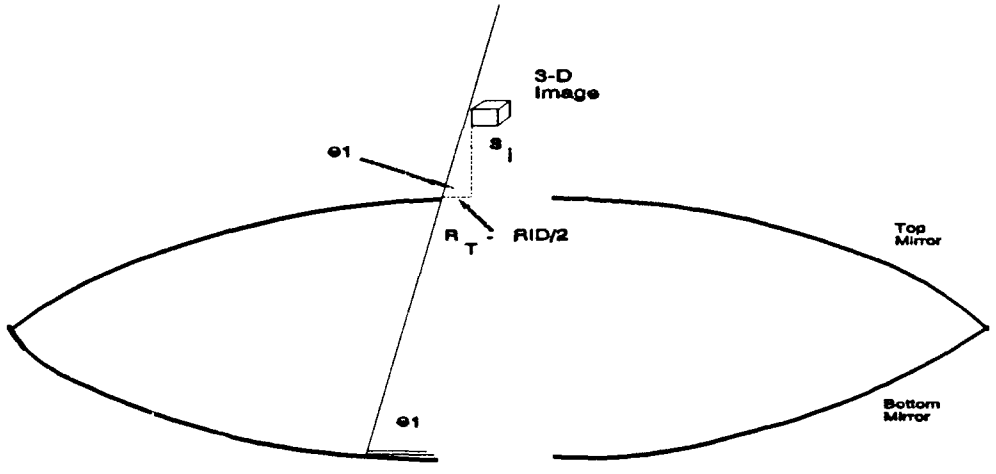

Figure B.3 Graphical explanation of the angle term Θ1.

$$\Theta 1_{min} = \tan^{-1}\frac{h}{R_{BM} - R_T} \qquad (B.1)$$

$$\therefore \Theta 1_{min} = 24.2^{\circ}$$

The angle $\theta 1$ is shown in Figure B.3 and is described by equation B.2. The angle $\theta 1$ exists within the range $\theta 1_{min} \leq \theta 1 \leq \theta 2$. The equation is a function of two variables, s_i and *RID* where again R_T is the radius of the hole in the top mirror, *RID* is the radius of the real image, and s_i is the distance that the top of the three-dimensional real image is located above the hole in the top mirror.

$$\theta 1 = \tan^{-1} \frac{s_i}{R_T - RID/2}$$

$$\therefore \theta 1 = \tan^{-1} \frac{s_i}{3.1 - RID/2} \qquad \text{(B.2)}$$

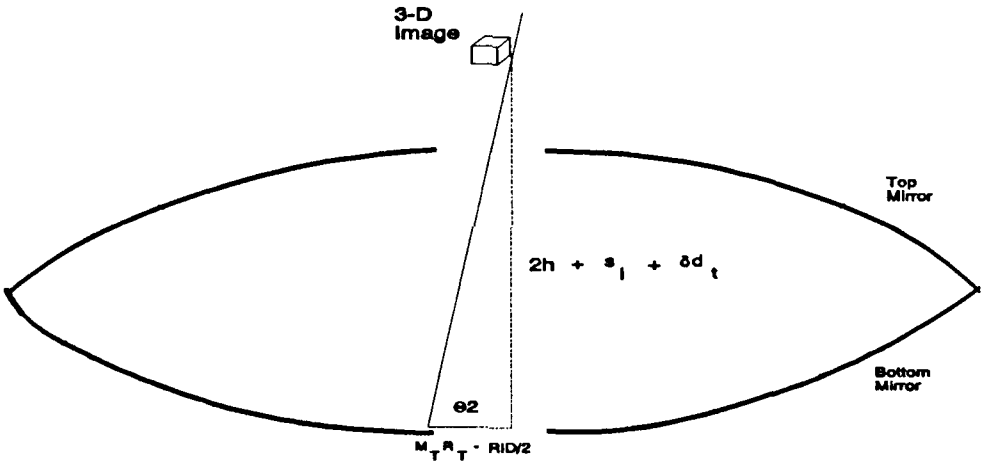

Figure B.4 Graphical explanation of the angle term $\theta 2$.

From Figure B.4, $\theta 2$ is formed by the line connecting the edge of the bottom hole to the opposite edge of the real image floating at the top of the two mirror system. It is simply derived from the triangle whose hypotenuse is formed by the ray starting from the edge of the image of the top hole on the bottom mirror to the edge of the image closest to the observer. The image of the top hole on the bottom mirror is easily calculated using a modified version of equation A.8 and A.9. The MATHCAD file TCMP.MCD in Appendix E performs this analysis. The result is

that the radius of the image of the top hole on the bottom mirror is 3.4 cm.

Another important variable to be considered in the mathematical description of the angle $\theta 2$ is the inclination angle of the image, β. Note that the graphical depictions of the angle terms shown in Figures B.2 through B.4 imply that the orientation of the images is parallel to the plane of the top hole of the two concave mirror projector. The two setups used in this experiment project a real image that is at a specific inclination angle from this parallel plane. The inclination angle of the image has a direct effect on the field of view of the two mirror system. Figure B.5 shows how the inclination angle affects the angle terms. This figure also shows the assumption that the image pivots at the edge tangent to the ray describing $\theta 1$. This simplifies the math by making $\theta 1$ independent of the inclination angle. Therefore, the angle $\theta 2$ is the only term dependent on the inclination angle, β.

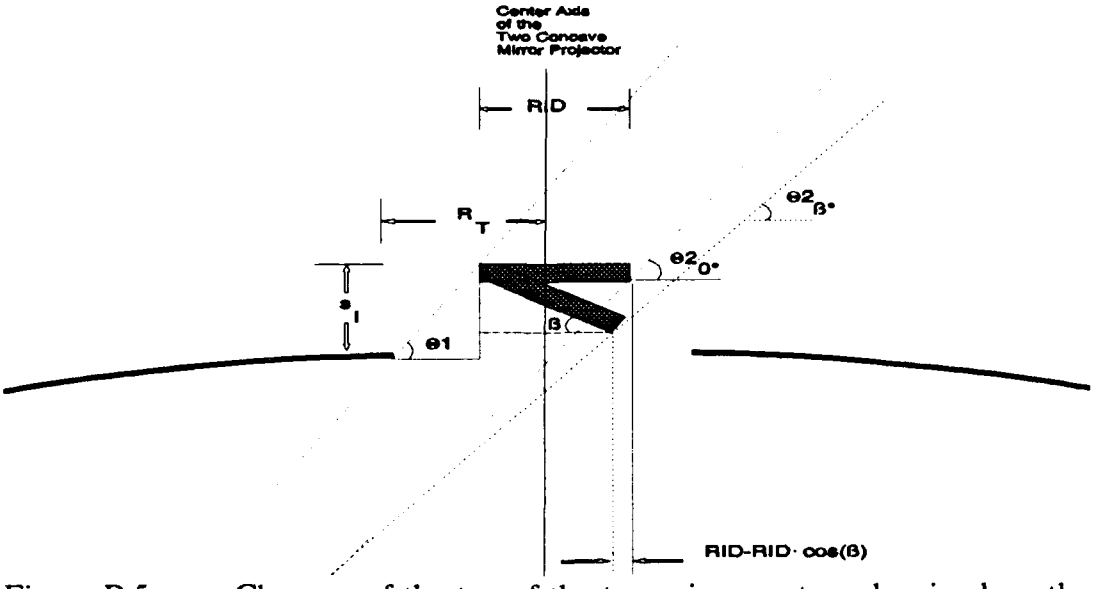

Figure B.5 Close-up of the top of the two mirror system showing how the rays defining the field of view angle terms are affected by an inclination of the image.

The angle $\theta 2$ is described by equation B.3.

$$\theta 2 = \tan^{-1} \frac{2h + \delta d_t + s_i - RID \cdot \sin(ß)}{M_T \cdot R_T + RID(\cos(ß) - 1/2)} \qquad (B.3)$$

$$\therefore \theta 2 = \tan^{-1} \frac{s_i - RID \cdot \sin(ß) + 7.5}{RID(\cos(ß) - 1/2) + 3.4}$$

where the term $2h$ represents the distance from the edge of the top hole to the edge of the bottom hole in the two concave mirror projector, and δd_t is the distance from the edge of the hole in the top mirror to the mirror apex. From Appendix A, δd_t is .29 cm.

Finally, the angle $\theta 2_{max}$ is formed by the line connecting the edge of the bottom hole to the centerline of the two mirror system and it is a fixed parameter that is derived from the equation for $\theta 2$. The only difference is that the variable s_i has been substituted with its equivalent for this case $R_t \tan(\theta 1_{min})$. Figure B.6 shows the geometry that makes up this angle. Equation B.4 shows the relation and numerical value for $\theta 2_{max}$.

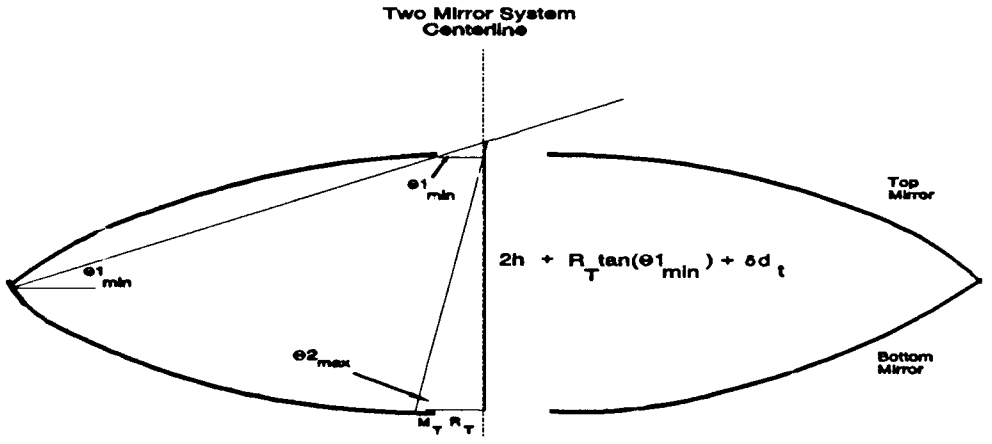

Figure B.6 Graphical explanation of the angle term $\theta 2_{max}$.

The field of view can be described using the four angles that have been defined. If the real image is a point that forms at the intersection of the $\theta 1_{min}$ and

$$\Theta 2_{max} = \tan^{-1} \frac{2h + \delta d_t + R_T \tan(\Theta 1_{min})}{M_T \cdot R_T} \qquad \text{(B.4)}$$

$$\therefore \Theta 2_{max} = 69.1°$$

$\Theta 2_{max}$ lines with the centerline of the system, the field of view is maximized and the result is FOV_{max}. On the other hand, if the real image forms at an arbitrary location above the plane of the hole, the field of view becomes smaller and is given by FOV.

The angles that make up FOV_{max} are $\Theta 1_{min}$ and $\Theta 2_{max}$. Likewise, the angles that make up FOV are $\Theta 1$ and $\Theta 2$.

Mathematically, FOV_{max} and FOV are described by B.5.

$$FOV_{max} = \Theta 2_{max} - \Theta 1_{min}$$
$$FOV = \Theta 2 - \Theta 1 \qquad \text{(B.5)}$$

The field of view is a function of the real image diameter, RID, and the location of the top of the three-dimensional real image, s_i. The terms R_T, R_{BM}, and h are fixed for this two mirror system, which in turn yielded fixed values for $\Theta 1_{min}$ and $\Theta 2_{max}$.

Therefore, by combining the results from equations B.1 through B.4 with the two equations in equation B.5, the numerical value for FOV_{max} and the equation for the FOV can be stated for the two concave mirror projector as

$$FOV_{max} = 44.9°$$

$$FOV = \tan^{-1} \frac{s_i - RID \cdot \sin(\beta) + 7.5}{RID(\cos(\beta) - 1/2) + 3.4} - \tan^{-1} \frac{s_i}{3.1 - RID/2} \qquad \text{(B.6)}$$

These results can be used as a check during the design process for the 3-D

display. The numerical value of the field of view equation must be positive in order for the viewer to see the real image.

The MATHCAD files, SYSTEM4.MCD and TCMP.MCD, use equation B.6 in their field of view analysis for the lens relay/two concave mirror projector setup and the diffuser/two concave mirror projector setup, respectively. Hardcopies of these files are located in Appendix E.

Appendix C. Criteria for Comfortable Viewing of the Lens Relay/Two Concave Mirror Projector Combination 3-D Display

The success of the 3-D display using the lens relay/two concave mirror projector combination does not rely solely on producing a real image at the top of the two concave mirror projector. The success also lies in producing this real image so that it does not cause discomfort for the viewer. This section will discuss the system parameters that affect the viewing comfort.

During the design of this 3-D display, it became evident that a comfort criteria was necessary after developing terrible headaches from staring at the display. Before going into an explanation of what caused this discomfort, it would be best to first define two key characteristics of the human visual system.

> 1. Accommodation. The degree of muscular effort required to focus the lens of the eye.
>
> 2. Convergence. In order to fuse the two images, each eye must rotate so that the point of interest is imaged onto corresponding points of each retina.
>
> (Veron, 1990)

The discomfort that was experienced in the early design phase of the 3-D display was a result of a conflict between accommodation and convergence. Figure C.1 shows how this conflict occurs. The viewer's eyes are both offset from the center of the optical system by *ES/2*. The field of view of each eye looking at the real image is represented by the two cones. The lens, which in this case is also the aperture stop

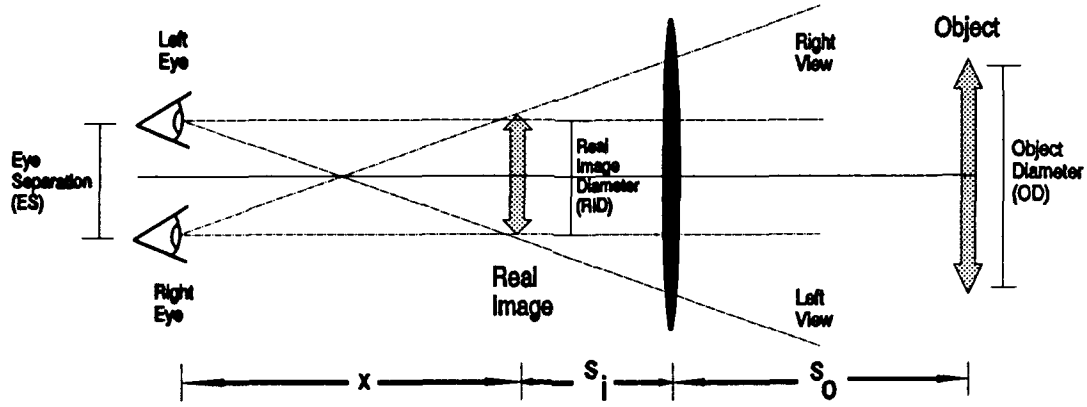

Figure C.1 Depiction of how the viewer's left and right eye converge on a real image floating in front of an optical element of finite size.

of this example, has a diameter of D_{AS}. Since the viewer is looking at a lens, his eyes will accommodate and converge to that lens as a display surface. When a real image is formed at a distance s_i from the lens, the left and right eye of the viewer must converge on that image as a point of interest. The image has a diameter of *RID*.

Comfortable viewing occurs when the viewer can see the real image with both his left and right eye simultaneously. If the size and location of the real image changes such that parts of the real image appear to disappear outside the physical dimensions of the lens, the viewer's eyes must converge more than normal to bring the full image back into view for each eye. This forced convergence while trying to remain accommodated on the lens as the display surface causes the discomfort to the viewer.

Once the cause of the discomfort was realized, a suitable equation had to be developed to help design comfort into the 3-D display. Referring again to Figure C.1, simple geometry solves the problem to ensure that the outer boundaries of the field of view for each eye looking at the image remains within the physical dimensions

of the lens. The result of this geometrical analysis is the comfort criteria shown in equation C.1.

$$\frac{x(FOVT \cdot D_{AS} - RID)}{s_1(ES + RID)} = 1 \qquad (C.1)$$

The term *FOVT*, which stands for the field of view tolerance, is added to give the criteria some flexibility. The *FOVT* has the range $RID/D_{AS} \leq FOVT \leq 1$. What this

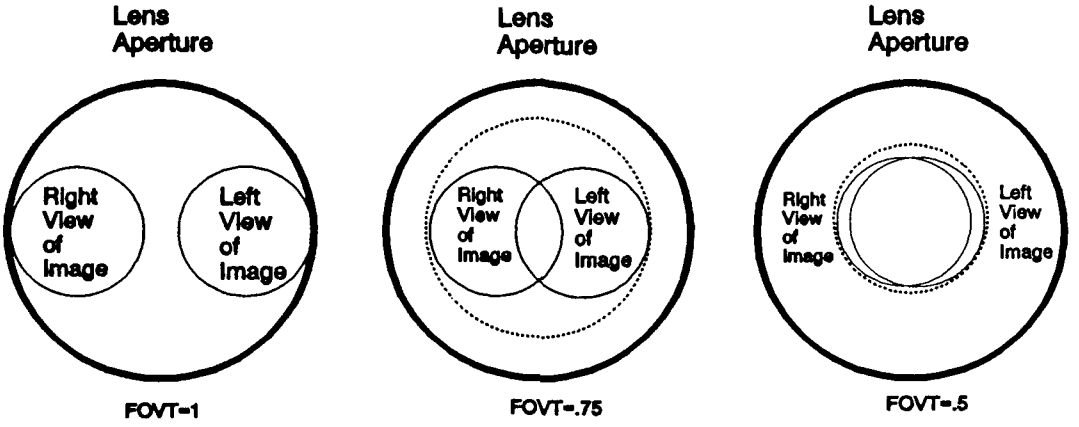

Figure C.2 Depiction of how the relative position of the left and right view of an image changes with a change in the field of view tolerance.

term does in the comfort criteria is that it allows the designer of the 3-D display to determine where the boundary of the field of view for each eye looking at the real image lies on the face of the aperture stop or the lens in this case. For example, when $FOVT=1$ the boundary of the field of view from each eye hits the outer edge of the lens, and when $FOVT=RID/D_{AS}$ the boundary of the field of view from each eye overlap at the center of the lens. Figure C.2 shows how the *FOVT* changes what the viewer sees when looking at the real image with the lens in the background.

The comfort criteria can be easily arranged to solve for any one variable. In

the case of the 3-D display design, the image location, x, the real image diameter, *RID*, the diameter of the aperture stop, D_{AS}, the field of view tolerance, *FOVT*, and the eye separation, *ES*, are given parameters. Therefore, the equation above can be rearranged to solve for the resulting minimum viewer distance, x.

$$x = \frac{s_i (ES + RID)}{FOVT \cdot D_{AS} - RID} \qquad (C.2)$$

This is the comfort equation used in the design MATHCAD file called *SYSTEM4.MCD*. A hard copy of the file is located in Appendix E.

Appendix D. Using the Available Resources

This appendix gives an overview of the techniques, equipment, and software that are available and necessary in order to achieve a working 3-D display. The specific areas to be covered are the Silicon Graphics Iris workstation, the 1" CRT, and finally existing 3-D software.

D.1 The Silicon Graphics Workstation

The Silicon Graphics Iris workstations that are available for image processing are located in the signal information processing lab, room 2011, Bldg. 642. Two types of workstations are available. The lab contains five 3000 series workstations and three 4D workstations.

The 3000 series workstations are older and do not have the superior window environment of the more modern 4D workstation. Because the 4D systems are in high demand, both systems have to be learned to maintain flexibility for working purposes. But when available, the 4D workstation has superior graphics capabilities.

Both systems operate in the UNIX environment. In fact, the first window that appears after logging in is called *console*. When working on the 3000 series, it is necessary to know the UNIX commands to get around. Some of the common UNIX commands are shown in Table D.I. The 4D on the other hand uses icons in a nice window environment to get around. The window environment in the 4D must be activated by clicking the RIGHT mouse button on the *system* icon and selecting *workspace*.

Table D.I Typical UNIX Commands.

Command	Description
cat *file1*	Catenate and print file1.
cd *directory*	Change to one of your directories.
cd ~*directory*	Change to another user's directory.
cp *file1 file2*	Copy file1 to file2.
cp *file1 ...dir*	Copy file1 to a new directory.
h	Shows history of commands executed.
lpr *file1*	Prints file1 to default printer.
lpr -P*printer f1*	Prints f1 to specified printer.
ls *name*	Lists the contents of a directory.
mkdir *directory*	Makes a new directory.
more *file1* View	file1 on screen by page.
mv *file1 file2*	Renames file1 as file2.
mv *file1 ...dir*	Moves file1 to a new directory.
pwd	Shows current directory pathname.
rmdir *directory*	Removes an old directory.
!#	Executes line # from command history.
!*char*	Executes latest command from history that starts with *char*.

Although the 4D has a superior window environment, the 3000 series does offer a multiple window environment called *mex*, which stands for Multiple Exposure. To enter this environment, type *mex* at the prompt. After this, the mouse will become enabled and you can *add* or *kill* a window at any time using the LEFT mouse button. Multiple windows give the ability to view more than one application at a time. It also is an ideal environment when writing source code. The source code can be displayed in one window while in the editor and the compiling and execution of the program can be done in a separate window without having to exit the editor. This is useful for troubleshooting source code.

D.2 1" CRTs

The three-dimensional perspective of the computer generated object can be displayed on either the Silicon Graphics Iris screen or on three 1" CRTs. The 1"

CRTs can be driven by the Silicon Graphics Iris workstation with an RGB output and sync. For this thesis effort, the Silicon Graphics Iris 4D workstation, Raphael, was used. Each CRT is monochrome. One is red, one is blue and the other is green. The workstation has an A→B video-switch that allows the user to send computer images to the screen or to the 1" CRTs. In the A position the image is sent to the screen. Likewise, in the B position the image is sent to the 1" CRTs.

The 1" CRTs are driven by a video driver that requires a different format from the Silicon Graphics than the format it normally sends to the screen. As a result, two different programs need to be run when switching between the screen and the 1" CRTs. The first program is called *SET60* and the second program is called a *SETNTSC*. The source code for these programs are located in the directory */usr/fac/amburn/src/sgi/misc*. When the video-switch is set to B, the program *SETNTSC* must be run for the image to appear on the 1" CRTs. When the video-switch is set to A, the program *SET60* must be run to return the video format back to normal for screen viewing.

The drawback of following the sequence described above is that between *SETNTSC* and *SET60* the commands need to be typed into the Silicon Graphics without being able to view it on the screen.

One other consideration must be taken care of in order for the computer generated image to appear on the face of the 1" CRTs. The window where the image is displayed on the computer screen must be in the lower left hand quarter. Otherwise, the image will not show up on the face of the 1" CRTs when you enter the NTSC mode and change the video-switch to the B position.

D.3 Existing Three-Dimensional Software

Programs for producing three-dimensional objects on a computer screen exist in different directories on the Silicon Graphics. The demos resident on the Silicon Graphics Iris 4D workstation were used for this thesis effort. The nice thing about these programs was that they generated the objects with the required perspective discussed in Chapter 2 to produce the three-dimensional effect. The demos used shading, motion and removal of hidden surfaces to produce this compelling effect.

The demos are easily accessible through the 4D workstation. After logging in, a *demos* icon appears as one of the choices in the upper left hand corner. Clicking the RIGHT mouse button on this icon will produce a list of available demos. Any one demo will work well.

Appendix E. MATHCAD Files Used During the 3-D Display Design Process

This section contains hardcopies of the MATHCAD files that were used to find the optical parameters of the two concave mirror projector (OPTIPARM.MCD), to find the size and location of a real image formed at the top of the two concave mirror projector when a solid object is place at the bottom (TCMP.MCD), and to find the required alignment of the optical components for the relay/two concave mirror projector combination (SYSTEM4.MCD).

E.1 OPTIPARM.MCD

This MATHCAD file finds the focal length of the top and bottom mirror as well as the distance separating the two mirrors that make up the two concave mirror projector. The file analyses the two cases discussed in Appendix A. The first case treats the mirrors as parabolic and solves the parameters based on this. The optical parameters calculated in this case are the actual values that were used in the design of the 3-D display.

The other case treated the mirrors as spherical in shape and the parameters were solved based on this. Notice that the calculated focal length is very different from the parabolic case even when the spherical degree, n, is 1.

CALCULATING THE OPTICAL PARAMETERS OF THE TWO CONCAWE MIRROR PROJECTOR

This MATHCAD file models the mirrors of the two concave mirror projector as either parabolic or spherical in shape. CASE I analyzes the top and bottom mirror as parabolic. CASE II analyzes the mirrors as spherical. Both analyses calculate the focal lengths of both mirrors and their separation distance based on physical dimensions of the mirrors.

First, we must define the physical dimensions of the two mirrors that will be used by both cases.

$x := -25 \ldots 25$	cm	The range for the x axis values	
$h_t := 3.6$	cm	h.t and h.b are the heights measured from the edge of the mirrors to the edge of the holes on the respective mirrors.	
$h_b := 3.6$	cm		
$x_{t1} := 3.1$	cm	x.t1 and x.b1 are the x values measured from the center axis of the mirrors to the edge of the holes on the top and bottom mirror.	
$x_{b1} := 3.0$	cm		
$x_{t2} := 11.3$	cm	x.t2 and x.b2 are the x values measured from the center axis of the mirrors to the edge of the the top and bottom mirror.	
$x_{b2} := 11.1$	cm		

CASE I. Assume that the mirrors are parabolic.

The mathematical description of the mirrors for this parabolic case is described by P.t(x,f.t) for the top mirror and P.b(x,f.b) for the bottom mirror.

$$P_t\left[x, f_t\right] := \frac{x^2}{4 \cdot f_t} \qquad P_b\left[x, f_b\right] := \frac{x^2}{4 \cdot f_b}$$

where f.t, f.b, and d are the unknown parameters representing the focal lenghts of the top and bottom mirror and the distance separating them, respectively.

Now the MATHCAD root function can be used to solve for these unknown variables. The root function will iterate the value of f.t and f.b until the relationships contained in the brackets are true. These relationships merely state that

the difference between the y values, P.t(x.t2,f.t) and P.t(x.t1,f.t) must equal the measured quantity h.t for the top mirror, and the difference between P.b(x.b2,f.b) and P.b(x.b1,f.b) must equal h.b for the bottom mirror.

Once the focal lengths have been calculated, the distance, d, separating the two mirrors can be calculated by adding the y values P.t(x.t2,f.t) and P.b(x.b2,f.b).

$f_t := 1\ cm \quad f_b := 1\ cm$ Guess values

$f_{top}[f_t] := root[P_t[x_{t2}, f_t] - P_t[x_{t1}, f_t] - h_t, f_t]$

$f_t := f_{top}[f_t]$

$f_{bot}[f_b] := root[P_b[x_{b2}, f_b] - P_b[x_{b1}, f_b] - h_b, f_b]$

$f_b := f_{bot}[f_b]$

$d := P_t[x_{t2}, f_t] + P_b[x_{b2}, f_b]$

The distance separating the parabolic mirrors is

$d = 7.78$ cm

The focal length of the top parabolic mirror is

$f_t = 8.2$ cm

The focal length of the bottom parabolic mirror is

$f_b = 7.93$ cm

CASE II. Assume that the mirrors are spherical to a degree controlled by n.

The mathematical description of the mirrors for this spherical case is described by S.t(x,f.t) for the top mirror and S.b(x.f.b) for the bottom mirror. The quantity n controls the spherical degree of the mirrors. Again, f.t, f.b, and d are the unknown parameters to be solved.

$$n := 0 \,..\, 1$$

$$f_t := 2 \qquad f_b := 2 \qquad \text{Guess Values}$$

$$S_t\left[x, f_t\right] := \sum_n \left[\frac{x^{2\cdot n+2}}{2^{n+1}\cdot (n+1)!\cdot \left[\frac{f_t}{2}\right]^{2\cdot n+1}} \right]$$

$$S_b\left[x, f_b\right] := \sum_n \left[\frac{x^{2\cdot n+2}}{2^{n+1}\cdot (n+1)!\cdot \left[\frac{f_b}{2}\right]^{2\cdot n+1}} \right]$$

Again, the MATHCAD root function can be used to solve for these unknown variables. The root function will iterate the value of f.t and f.b until the relationships contained in the brackets are true. These relationships merely state that the difference between the y values, S.t(x.t2,f.t) and S.t(x.t1,f.t) must equal the measured quantity h.t for the top mirror, and the difference between S.b(x.b2,f.b) and S.b(x.b1,f.b) must equal h.b for the bottom mirror.

Once the focal lengths have been calculated, the distance, d, separating the two mirrors can be calculated by adding the y values S.t(x.t2,f.t) and S.b(x.b2,f.b).

$$f_{top}\left[f_t\right] := root\left[S_t\left[x_{t2}, f_t\right] - S_t\left[x_{t1}, f_t\right] - h_t, f_t\right]$$

$$f_t := f_{top}\left[f_t\right]$$

$$f_{bot}\left[f_b\right] := root\left[S_b\left[x_{b2}, f_b\right] - S_b\left[x_{b1}, f_b\right] - h_b, f_b\right]$$

$$f_b := f_{bot}\left[f_b\right]$$

$$d := S_t\left[x_{t2}, f_t\right] + S_b\left[x_{b2}, f_b\right]$$

The distance separating the two spherical mirrors is

$$d = 7.73 \quad \text{cm}$$

The focal length of the top spherical mirror is

$$f_t = 36.23 \quad \text{cm}$$

The focal length of the bottom spherical mirror is

$$f_b = 35.12 \quad \text{cm}$$

E.2 TCMP.MCD

This MATHCAD file is broken into three parts. The first part uses equation A.8 and A.9 to predict the location and size of the real image that forms at the top of the two concave mirror projector when a solid object is placed at the bottom. In this example, the location and size of the diffuser is calculated. This part was also used during the verification of the focal lengths of the top and bottom mirror in Appendix A.

The second part calculates the size of the image of the top hole on the bottom mirror. This is a crucial physical quantity that determines the field of view angle $\theta 2$. This is discussed in greater detail in Appendix B.

The third part uses equation B.6 to calculate the field of view of an image with known size, location, and inclination. The size and location of the image and the field of view calculation shown on the hardcopy represent the actual values for the successful demonstration of the diffuser/two concave mirror projector setup.

Real Image Prediction for the Two Concave Mirror Projector

This MATHCAD file is broken up into three parts. The first part uses equations A.8 and A.9 derived in Appendix A to describe the size and location of the real image generated by the two concave mirror projector. The second part calculates the size of the image of the top hole on the bottom mirror. This is a necessary quantity for the field of view calcualtion. Finally, the third part calculates the field of view for this image.

PART I. The Two Concave Mirror Projector as an Imaging System.

The given values for the focal length of the top and bottom mirror, f.t and f.b, respectively, the separation distance between the mirrors, d, the distance on the cavity side that the object is from the bottom hole, s.o, and the distance that the top and bottom hole are from the apex of their respective mirror, $d.t and $d.b, respectively, are defined below.

$f_t \equiv 8.2$ cm $\quad f_b \equiv 7.9$ cm

$d \equiv 7.8$ cm $\quad s_o \equiv .75$ cm

$\$d_t \equiv .29$ cm $\quad \$d_b \equiv .29$ cm

Equation A.8 calculates the distance, s.i, that the image forms from the top of the two concave mirror projector. The equation is stated below:

$$s_i := \frac{d\cdot\left[f_b - A\right] + f_b\cdot A + \dfrac{B\cdot\left[f_t\cdot A - f_t\cdot f_b\right]}{B - f_t}}{d - f_b - \dfrac{f_t\cdot B}{B - f_t}}$$

where

$A \equiv d - \$d_t$

$B \equiv d - \$d_b - s_o$

The resulting image location is

$$s_i = 2.02 \quad cm$$

Equation A.9 calculates the magnification, M.T, of this image. It is stated below along with its result.

$$M_T := \frac{f_t \cdot \left[s_i + d - \delta d_t \right]}{d \cdot \left[s_o - f_t \right] - s_o \cdot f_t} \qquad M_T = -1.22$$

PART II. Calculation of the image size of the top hole on the bottom mirror.

This calculation is required to complete the calculation for the field of view. The two mirror system images the top hole on the bottom mirror. As a result, the field of view angle, $\theta 2$, is measured from the edge of this image.

This calculation uses a slightly modified version of the two equations used above. In this case, we are looking through the two mirror system from the top instead of from the bottom. The location of the hole is at s.o=0.

$$s_o \equiv 0 \quad cm$$

Equation A.8 must be modified simply by swapping top mirror parameters for bottom mirror parameters and vice versa in the equation. The modified equation can be rewritten as

$$A := d - \delta d_b$$

$$B := d - \delta d_t - s_o$$

$$s_i := \frac{d \cdot \left[f_t - A \right] + f_t \cdot A + \dfrac{B \cdot \left[f_b \cdot A - f_t \cdot f_b \right]}{B - f_b}}{d - f_t - \dfrac{f_b \cdot B}{B - f_b}}$$

$$s_i = 1.13 \quad cm$$

The resulting magnification of the top hole image on the bottom mirror is calculated by the equation below. This equation is just a modified version of equation A.9, where again the top mirror parameters are swapped with the bottom mirror parameters.

$$M_T := \frac{f_b \cdot [s_i + d - \$d_b]}{d \cdot [s_o - f_b] - s_o \cdot f_b}$$

$M_T = -1.11$

Since we know that the diameter of the top hole is 6.2 cm, the image size of the top hole on the bottom mirror is

$D_{Ti} := |M_T| \cdot 6.2$ $\quad D_{Ti} = 6.87$ cm

The field of view equation requires the radius of the image as a parameter. This is easily calculated as

$$R_{Ti} := \frac{D_{Ti}}{2} \qquad R_{Ti} = 3.44 \text{ cm}$$

PART III. Calculation of the Field of View.

As the title implies, this section will calculate the field of view, using equation B.7 (see Appendix B), of an image. The image size and location are defined below.

RID := 1 in RID := RID·2.54

RID = 2.54 cm Image Diameter

$s_i := 2$ cm Image Location

From Appendix B, the field of view is a function of the diameter of the real image in the plane of the top hole of the two mirror system. If the image is angled with respect to this plane, the size of the projected diameter of the image becomes important.

The size of the projected diameter of the image to the horizontal plane of the two mirror system is a function of the inclination angle of the image, β.

$\beta := 60$ degrees

$$\beta := \beta \cdot \frac{\pi}{180} \quad \text{radians}$$

From equation B.6, the maximum field of view subtended by the two concave mirror projector for this image is

$$\theta 2 := \operatorname{atan}\left[\frac{s_i + 7.5 - RID \cdot \sin(\beta)}{RID \cdot (\cos(\beta) - .5) + R_{Ti}}\right]$$

$$\theta 1 := \operatorname{atan}\left[\frac{s_i}{3.1 - \frac{RID}{2}}\right]$$

$$FOV := (\theta 2 - \theta 1) \cdot \frac{180}{\pi} \qquad FOV = 17.26 \quad \text{degrees}$$

E.3 SYSTEM4.MCD

This MATHCAD file uses the comfort equation derived in Appendix C and the matrix technique discussed in Chapter 3 to design the optical relay that makes up the lens relay/two concave mirror projector combination.

The file uses the generic subsystem matrix defined in equation 3.7 and the maximum separation distance between elements, defined by equation 3.8, to find the maximum separation for all the optical components.

An iteration method is then used to find the required optical element separation to perform the desired imaging. The values for the maximum separation distance calculated using equation 3.8 are used as constraints during this iteration method.

The field of view of this display is calculated using the matrix technique and the field of view equation. Since the field of view is determined by the optical setup and not by the two mirror system alone, the field of view equation, eqn. B.6, gives an idea of what the limitations imposed by the two mirror system are, but the matrix technique tells what the actual field of view of the image floating at the top is.

The numerical values shown throughout this hardcopy apply to the actual setup used for the lens relay/two concave mirror projector setup.

The 3-D Display Design Using a Four Lens Relay

This MATHCAD file will help design a four optical element relay in combination with two concave mirror projector for my thesis effort. The file will take into account the comfort factor, and make sure the optics are arranged such that the last aperture in the two mirror projector is the aperture stop of the system.

The anaysis is broken up into two parts. The first part will calculate the maximum separation distances allowed between the optical elements to ensure the last aperture of the relay is the aperture stop of the system. The second part will alter these distances slightly to accomplish the required imaging while staying within the maximum allowable separation distance.

PART I. CALCULATE THE MAXIMUM SEPARATION DISTANCE BETWEEN ALL OPTICAL ELEMENTS.

Step 1. Declare all known optical parameters. This includes focal lengths, diameters, distance separating the two mirrors, and the minimum field of view boundary.

Lens #1: $f_1 := 15$ cm
$D_1 := 3$ in
$D_1 := D_1 \cdot 2.54$
$D_1 = 7.62$ cm

Lens #2: $f_2 := 10$ cm
$D_2 := 3$ in
$D_2 := D_2 \cdot 2.54$
$D_2 = 7.62$ cm

Lens #3: $f_3 := 10$ cm
$D_3 := 3$ in
$D_3 := D_3 \cdot 2.54$
$D_3 = 7.62$ cm

Lens #4: $f_4 := 6.29$ cm
$D_4 := 2$ in
$D_4 := D_4 \cdot 2.54$
$D_4 = 5.08$ cm

Object Diameter: $OD := 2$ in $OD := OD \cdot 2.54$
$OD = 5.08$ cm

Top Mirror:

$f_t := 8.2$ $D_t := 11.3$ cm

Bottom Mirror:

$f_b := 7.9$ $D_b := 11.1$ cm

Distance Separating the Mirrors: $d := 7.7$ cm
Size of the top hole: $D_T := 6.2$ cm

The minimum FOV boundary as measured from the vertical: $\theta1_{min} := 65.8$ degrees

$\theta1_{min} := \theta1_{min} \cdot \frac{\pi}{180}$ $\theta1_{min} = 1.15$ radians

Step 2: Use the comfort equation to find the required viewing distance from the location of the real image. The design of the relay will proceed backwards from this point.

The first step is to determine what the aperture stop is to the viewer, one must compare the minimum angle subtended by the two mirror system, $\theta1.min$, and the angle subtended by the image, $\alpha.i$.

es := 6.5 cm RID := 2 in
si := 2 cm RID := RID·2.54
FOVT := 1 RID = 5.08 cm

$$\alpha_i := \frac{\frac{D_T}{2} - \frac{RID}{2}}{si}$$

The next step is to determine if the aperture stop is the top hole or the bottom mirror.

$$D_{AS} := if\left[\alpha_i \geq \theta1_{min}, D_b, D_T\right]$$

The aperture stop is D.b if D.AS=11.1 or it is D.T if D.AS=6.2.

$D_{AS} = 6.2$ cm

$$x := \frac{(es + RID)\cdot si}{FOVT\cdot D_{AS} - RID} \qquad x = 20.68 \text{ cm}$$

Step 3. Find the maximum distances that the four lenses and the top mirror of two mirror system can be separated by to ensure that the top hole of two mirror system is the aperture stop.

I will use the matrix method here. The matrix is derived in the Chapter 3. The matrix below is a generic matrix which describes the propagation of a ray over a distance, d, then hitting an optical element with focal length, f. This generic matrix will be used throughout this analysis, and it is a function of d and f.

$$A(d,f) := \begin{bmatrix} 1 - \frac{d}{f} & -\frac{1}{f} \\ d & 1 \end{bmatrix}$$

Also, from here on, the analysis will trace the two key rays discussed in Chapter 3. The first ray mimics what the viewer would see if he were located at the image location, si. The second ray mimics what the viewer would see if he were in the far field, ∞.

a) The real image imaged through the bottom mirror. Find the ray parmeters, α and y, for both cases stated below.

CASE I. Viewer at si.

$di := si + d$

$$y_i := \frac{RID}{2}$$

$$\alpha_{i1} := \frac{\frac{D_{AS}}{2} - \frac{RID}{2}}{si}$$

$$\alpha_{i2} := \frac{\frac{D_b}{2} - \frac{RID}{2}}{di}$$

$$\alpha_i := if\left[\alpha_i \geq \theta 1_{min}, \alpha_{i2}, \alpha_{i1}\right]$$

$\alpha_i = 0.28$ $y_i = 2.54$ cm

$$\begin{bmatrix} \alpha_{ib} \\ y_{ib} \end{bmatrix} := A\left[di, f_b\right] \cdot \begin{bmatrix} \alpha_i \\ y_i \end{bmatrix}$$

$\alpha_{ib} = -0.39$

$y_{ib} = 5.26$ cm

CASE II. Viewer at ∞.

$d\infty := \infty$

$$y_\infty := \frac{D_T}{2}$$

$\alpha_\infty := 0$

$\alpha_\infty = 0$ $y_\infty = 3.1$ cm

$$\begin{bmatrix} \alpha_{\infty b} \\ y_{\infty b} \end{bmatrix} := A\left[d\infty, f_b\right] \cdot \begin{bmatrix} \alpha_\infty \\ y_\infty \end{bmatrix}$$

$\alpha_{\infty b} = -0.39$

$y_{\infty b} = 3.1$ cm

b) The resulting ray from above imaged through the top mirror. Find the ray parameters, $\propto$ and y, for both cases.

CASE I. Viewer at si.

$$\begin{bmatrix} \propto_{it} \\ y_{it} \end{bmatrix} := A\begin{bmatrix} d, f_t \end{bmatrix} \cdot \begin{bmatrix} \propto_{ib} \\ y_{ib} \end{bmatrix}$$

$\propto_{it} = -0.66$

$y_{it} = 2.29 \quad cm$

CASE II. Viewer at ∞.

$$\begin{bmatrix} \propto_{\infty t} \\ y_{\infty t} \end{bmatrix} := A\begin{bmatrix} d, f_t \end{bmatrix} \cdot \begin{bmatrix} \propto_{\infty b} \\ y_{\infty b} \end{bmatrix}$$

$\propto_{\infty t} = -0.4$

$y_{\infty t} = 0.08 \quad cm$

c) The resulting image from above imaged through Lens 4. Find the maximum allwoable distance between Lens 4 and the top mirror, d4.max, and the ray parameters, $\propto$ and y, for both cases.

CASE I. Viewer at si.

$$d4_i := \frac{\frac{-D_4}{2} - y_{it}}{\propto_{it}}$$

$d4_i = 7.27 \quad cm$

CASE II. Viewer at ∞.

$$d4_\infty := \frac{\frac{-D_4}{2} - y_{\infty t}}{\propto_{\infty t}}$$

$d4_\infty = 6.51 \quad cm$

$d4_{max} := if\left[d4_i \geq d4_\infty, d4_\infty, d4_i\right] \quad d4_{max} := d4_\infty \quad d4_{max} = 6.51$

$$\begin{bmatrix} \propto_{i4} \\ y_{i4} \end{bmatrix} := A\begin{bmatrix} d4, f_4 \end{bmatrix} \cdot \begin{bmatrix} \propto_{it} \\ y_{it} \end{bmatrix}$$

$\propto_{i4} = -0.34$

$y_{i4} = -2.04 \quad cm$

$$\begin{bmatrix} \propto_{\infty 4} \\ y_{\infty 4} \end{bmatrix} := A\begin{bmatrix} d4, f_4 \end{bmatrix} \cdot \begin{bmatrix} \propto_{\infty t} \\ y_{\infty t} \end{bmatrix}$$

$\propto_{\infty 4} = 0$

$y_{\infty 4} = -2.54 \quad cm$

d) The resulting ray from above imaged through Lens 3. Find the maximum allowable distance between Lens 3 and Lens 4, d3.max, and the ray parameters, $\propto$ and y, for both cases.

CASE I. Viewer at si.

$$d3_i := \frac{\frac{-D_3}{2} - y_{i4}}{\alpha_{i4}}$$

$d3_i = 5.2$ cm

$d3_{max} := if\left[d3_i \geq d3_\infty, d3_\infty, d3_i\right]$

$$\begin{bmatrix} \alpha_{i3} \\ y_{i3} \end{bmatrix} := A\left[d3, f_3\right] \cdot \begin{bmatrix} \alpha_{i4} \\ y_{i4} \end{bmatrix}$$

$\alpha_{i3} = 0.04$

$y_{i3} = -3.81$ cm

CASE II. Viewer at ∞.

$$d3_\infty := \frac{\frac{D_3}{2} - y_{\infty 4}}{\alpha_{\infty 4}}$$

$d3_\infty = 3.45 \cdot 10^3$ cm

$d3 := d3_{max}$ $d3 = 5.2$

$$\begin{bmatrix} \alpha_{\infty 3} \\ y_{\infty 3} \end{bmatrix} := A\left[d3, f_3\right] \cdot \begin{bmatrix} \alpha_{\infty 4} \\ y_{\infty 4} \end{bmatrix}$$

$\alpha_{\infty 3} = 0.25$

$y_{\infty 3} = -2.53$ cm

e) The resulting ray from above imaged through Lens 2. Find the maximum allowable distance between Lens 2 and Lens 3, d2.max, and the ray parameters, ∝ and y, for both cases.

CASE I. Viewer at si.

$$d2_i := \frac{\frac{D_2}{2} - y_{i3}}{\alpha_{i3}}$$

$d2_i = 187.02$ cm

$d2_{max} := if\left[d2_i \geq d2_\infty, d2_\infty, d2_i\right]$

$$\begin{bmatrix} \alpha_{i2} \\ y_{i2} \end{bmatrix} := A\left[d2, f_2\right] \cdot \begin{bmatrix} \alpha_{i3} \\ y_{i3} \end{bmatrix}$$

$\alpha_{i2} = 0.32$

CASE II. Viewer at ∞.

$$d2_\infty := \frac{\frac{D_2}{2} - y_{\infty 3}}{\alpha_{\infty 3}}$$

$d2_\infty = 24.88$ cm

$d2 := d2_{max}$ $d2 = 24.88$

$$\begin{bmatrix} \alpha_{\infty 2} \\ y_{\infty 2} \end{bmatrix} := A\left[d2, f_2\right] \cdot \begin{bmatrix} \alpha_{\infty 3} \\ y_{\infty 3} \end{bmatrix}$$

$\alpha_{\infty 2} = -0.13$

$y_{i2} = -2.8 \quad cm$ $y_{\infty 2} = 3.81 \quad cm$

f) The resulting ray from above imaged through Lens 1. Find the maximum allowable distance between Lens 1 and Lens 2, d1.max, and the ray parameters, α and y, for both cases.

CASE I. Viewer at si.

$$d1_i := \frac{\frac{D}{2} - y_{i2}}{\alpha_{i2}}$$

$d1_i = 20.62 \quad cm$

CASE II. Viewer at ∞.

$$d1_\infty := \frac{\frac{-D}{2} - y_{\infty 2}}{\alpha_{\infty 2}}$$

$d1_\infty = 60.42 \quad cm$

$d1_{max} := if\left[d1_i \geq d1_\infty, d1_\infty, d1_i\right]$ $d1 := d1_{max}$ $d1 = 20.62$

$$\begin{bmatrix} \alpha_{i1} \\ y_{i1} \end{bmatrix} := A\left[d1, f_1\right] \cdot \begin{bmatrix} \alpha_{i2} \\ y_{i2} \end{bmatrix}$$

$\alpha_{i1} = 0.07$

$y_{i1} = 3.81 \quad cm$

$$\begin{bmatrix} \alpha_{\infty 1} \\ y_{\infty 1} \end{bmatrix} := A\left[d1, f_1\right] \cdot \begin{bmatrix} \alpha_{\infty 2} \\ y_{\infty 2} \end{bmatrix}$$

$\alpha_{\infty 1} = -0.21$

$y_{\infty 1} = 1.21 \quad cm$

PART II. FIND THE REQUIRED OPTICAL ELEMENT SEPARATION DISTANCES TO ACCOMPLISH THE REQUIRED IMAGING.

The system must image an object of diameter OD to an image plane located a distance si from the aperture stop. The diameter of the image is RID. These variables were defined in PART I and apply here.

Step 1. The first step is to define a system matrix for a ray propagating backwards through the relay from the image plane to the other side of Lens #1. The system matrix is a function of the three separation distances--d1, d2, and d3. The reason only these three functions have been chosen is because d4 and d have no physical flexibility.

The system matrix function is broken up into a fixed part and variable part:

$$S_{fix} := A\left[d4, f_4\right] \cdot A\left[d, f_t\right] \cdot A\left[di, f_b\right]$$

$$S(d1,d2,d3) := A\left[\begin{matrix} d1, f_1 \end{matrix}\right] \cdot A\left[\begin{matrix} d2, f_2 \end{matrix}\right] \cdot A\left[\begin{matrix} d3, f_3 \end{matrix}\right] \cdot S_{fix}$$

Step 2. The next step is to propagate two rays from the same point on the image but at different angles through the relay and find the angle and height of these rays as they emerge from the face of Lens #1.

A ray matrix function whose elements are $\alpha.t1$ and $y.t1$ is defined below. These individual elements are extracted in the following two lines. $\alpha.t1$ and $y.t1$ represent the angle and height of the ray emerging from the face of Lens #1. The ray entering the relay has and angle $\alpha.i$ and a height $y.i$.

$$RAY1(d1,d2,d3) := S(d1,d2,d3) \cdot \begin{bmatrix} \alpha_i \\ y_i \end{bmatrix}$$

$$\alpha_{t1}(d1,d2,d3) := RAY1(d1,d2,d3) \cdot \begin{bmatrix} 1 \\ 0 \end{bmatrix}$$

$$y_{t1}(d1,d2,d3) := RAY1(d1,d2,d3) \cdot \begin{bmatrix} 0 \\ 1 \end{bmatrix}$$

A second ray matrix function whose elements are $\alpha.t2$ and $y.t2$ is defined below with the individual elements extracted in the following two lines. $\alpha.t2$ and $y.t2$ represent the angle and height of the ray emerging from the face of Lens #1. The ray entering the relay has and angle of 0 and a height $y.i$.

$$RAY2(d1,d2,d3) := S(d1,d2,d3) \cdot \begin{bmatrix} 0 \\ y_i \end{bmatrix}$$

$$\alpha_{t2}(d1,d2,d3) := RAY2(d1,d2,d3) \cdot \begin{bmatrix} 1 \\ 0 \end{bmatrix}$$

$$y_{t2}(d1,d2,d3) := RAY2(d1,d2,d3) \cdot \begin{bmatrix} 0 \\ 1 \end{bmatrix}$$

Step 3. This step defines the distance in front of Lens #1 where each of the two rays defined above travel until they reach a height of OD/2.

$$sol1(d1,d2,d3) := \frac{\frac{OD}{2} - y_{t1}(d1,d2,d3)}{\propto_{t1}(d1,d2,d3)}$$

$$so2(d1,d2,d3) := \frac{\frac{OD}{2} - y_{t2}(d1,d2,d3)}{\propto_{t2}(d1,d2,d3)}$$

Step 4. This step uses the SOLVE BLOCK function in MATHCAD to find the required optical element separations d1, d2, and d3. Plugging these values back into sol(d1,d2,d3) will give the required object distance.

The key to this solution method is to require that sol(d1,d2,d3) equal so2(d1,d2,d3). This forces the two rays that entered the system to intersect at a common point in the object plane.

Given

$sol1(d1,d2,d3) \approx so2(d1,d2,d3)$

The following constraints must be declared in order to prevent the solver from picking a separation distance greater than the maximum allowable or less than zero. It will also prevent the object distance from being less than zero.

$d1 \leq d1_{max}$ $\quad d2 \leq d2_{max}$ $\quad d3 \leq d3_{max}$ $\quad sol1(d1,d2,d3) \geq 0$

$d1 \geq 0$ $\quad d2 \geq 0$ $\quad d3 \geq 0$ $\quad so2(d1,d2,d3) \geq 0$

The solution can now be found by the function shown below (NOTE: IF THE ERROR FLAG "DID NOT FIND SOLUTION" APPEARS, THE INITIAL CONDITIONS MUST BE CHANGED).

$$\begin{bmatrix} d1 \\ d2 \\ d3 \end{bmatrix} := Find(d1,d2,d3) \qquad so := sol1(d1,d2,d3)$$

$so = 1.97 \cdot 10^{-5}$	cm	The object distance.
$d1 = 16.27$	cm	Distance separating L1 and L2.
$d2 = 16.48$	cm	Distance separating L2 and L3.
$d3 = 4.98$	cm	Distance separating L3 and L4.
$d4 = 6.51$	cm	Distance separating L4 and M.t.

$so + d1 + d2 + d3 + d4 = 44.25$ cm The total length of the system.

Step 5. This step performs a quick check on the values found above. It uses the matrix technique to find the resulting image location, si, based on the values above. If si is the same as what it was defined as in Part I, then the design is a success.

First, a system matrix for forward propagation has to be defined from the object plane to the plane of the top hole of the two mirror system.

$$P := A\left[\begin{matrix} d2, f_3 \end{matrix}\right] \cdot A\left[\begin{matrix} d1, f_2 \end{matrix}\right] \cdot A\left[\begin{matrix} so, f_1 \end{matrix}\right]$$

$$A := \begin{bmatrix} 1 & 0 \\ d & 1 \end{bmatrix} \cdot A\left[\begin{matrix} d, f_b \end{matrix}\right] \cdot A\left[\begin{matrix} d4, f_t \end{matrix}\right] \cdot A\left[\begin{matrix} d3, f_4 \end{matrix}\right] \cdot P$$

The next step is to propagate two rays originating from the same point on the object (y.o) but different angles ($\propto$.o1 and $\propto$.o2), and calculate where they intersect in the image plane.

$$y_o := \frac{OD}{2} \qquad \propto_{o1} := -\propto_{t1} \quad (d1, d2, d3) \qquad \propto_{o2} := 0$$

$$\begin{bmatrix} \propto_{i1} \\ y_{i1} \end{bmatrix} := A \cdot \begin{bmatrix} \propto_{o1} \\ y_o \end{bmatrix}$$

$\propto_{i1} = -0.28 \qquad y_{i1} = 3.1 \quad cm$

$y1(x) := \propto_{i1} \cdot x + y_{i1}$ This is the equation of the line formed by yi1 and $\propto$i1.

$$\begin{bmatrix} \propto_{i2} \\ y_{i2} \end{bmatrix} := A \cdot \begin{bmatrix} \propto_{o2} \\ y_o \end{bmatrix}$$

$\propto_{i2} = -0.1 \qquad y_{i2} = 2.73 \quad cm$

$y2(x) := \propto_{i2} \cdot x + y_{i2}$ This is the equation of the line formed by yi2 and $\propto$i2.

The two lines intersect where the image forms.

x := 1 Guess value

$si_x := root(y2(x) - y1(x), x)$ This function solves for x.

$si_x = 2$ cm $y2[si_x] = 2.54$ cm This is the height and location of the intersecting lines.

$si = 2$ cm $\frac{RID}{2} = 2.54$ cm This is what the height and location of the lines should be.

The field of view of the image calculated above can also be calculated. This is done by again using two rays.

The first ray is identical to the first ray defined above where the angle incident on Lens #1 was described by $\alpha.o1$ and the height was y.o. This ray then exited the top of the two mirror system with an angle $\alpha.i1$.

If a second ray is defined going from the opposite end of the object (negative value of y.o) and with an angle that is the negative of $\alpha.o1$, then one would expect this ray to exit the system with an angle that is the negative of $\alpha.i1$.

These two rays would exit the system tangentially to the image. Therefore, they form the boundary rays that define the field of view.

The field of view can therefore be defined by

$$FOV := 2 \cdot |\alpha_{i1}| \cdot \frac{180}{\pi} \qquad FOV = 32.09 \text{ degrees}$$

This quantity can be directly compared to the field of view equation derived in Appendix B.

From Appendix B, the field of view is a function of the diameter of the real image in the plane of the top hole of the two mirror system. If the image is angled with respect to this plane, the size of the projected diameter of the image becomes important.

The size of the projected diameter of the image to the horizontal plane of the two mirror system is a function of the inclination angle of the image, β.

$\beta := 45$ degrees

$$\beta := \beta \cdot \frac{\pi}{180} \quad \text{radians}$$

From equation B.6, the maximum field of view subtended by the two concave mirror projector for this image can be calculated.

The actual size of the image, not including the imaging of the background is

$$RID := 1 \quad in \qquad RID := RID \cdot 2.54$$

$$RID = 2.54 \quad cm$$

The field of view can be written in terms of the two angles that define it.

$$\theta 2 := \operatorname{atan}\left[\frac{si + 7.5 - RID \cdot \sin(\beta)}{RID \cdot (\cos(\beta) - .5) + 3.4}\right]$$

$$\theta 1 := \operatorname{atan}\left[\frac{si}{3.1 - \frac{RID}{2}}\right]$$

$$FOV := (\theta 2 - \theta 1) \cdot \frac{180}{\pi} \qquad FOV = 15.45 \quad degrees$$

Bibliography

Campbell, Jon. "Rotating Disk Produces Real 3D Images," Electronic Design, 29 (September 1990).

Clapp, Robert E. "Stereoscopic Perception," SPIE Vol. 761 True 3D Imaging Techniques and Display Technologies, 79-81 (January 1987).

Eichenlaub, Jesse B. "An Autostereoscopic Display for Use with a Personal Computer," SPIE Vol. 1256 Stereoscopic Displays and Applications, 156-163 (February 1990).

Free, John. "Digital Holography," Popular Science, 84-87 (January 1991).

Goodman, J. W. *Introduction to Fourier Optics.* San Francisco, California: McGraw-Hill, 1968.

Hariharan, P. *Optical Holography*. Cambridge: Cambridge University Press, 1984.

Hect, Eugene. *Optics--Second Edition.* Reading, Massachusetts: Addison-Wesley, 1988.

Kollin, Joel S. and others. "Real-Time Display of 3-D Computed Holograms by Scanning the Image of an Acousto-Optic Modulator," *SPIE Vol. 1136 Holographic Optics II: Principles and Applications*. 178-182. (April 1989).

Stuart, Capt Bryant L. *Computer Generated Holography as a Three-Dimensional Display Medium*. MS Thesis, AFIT/GCS/ENG/90D-14. School of Engineering, Air Force Institute of Technology (AU), Wright-Patterson AFB OH, December 1990.

Travis, Adrian R. L. "Autostereoscopic 3-D display," Applied Optics, Vol. 29 No. 29: 4341-4342 (October 1990).

Veron, H. and others. "Stereoscopic Displays for Terrain Database Visualization." SPIE Vol. 1256 Stereoscopic Displays and Applications, 2-11 (February 1990).

Wickens, Christopher D. "Three-dimensional stereoscopic display implementation: Guidelines derived from human visual capabilities," SPIE Vol. 1256 Stereoscopic Displays and Applications, 2-11 (February 1990).